NTNU – Trondheim
Norwegian University of
Science and Technology

Investigation of loss of surfactants during enhanced oil recovery applications - adsorption of surfactants onto clay materials

Eivind Joo Behrens

Chemical Engineering and Biotechnology
Submission date: June 2013
Supervisor: Gisle Øye, IKP

Norwegian University of Science and Technology
Department of Chemical Engineering

Preface

This thesis is submitted as a part of my MSc. Degree in Industrial Chemistry and Biotechnology at the Norwegian University of Science and Technology (NTNU).

The experimental work performed in context with this study has been carried out at the Ugelstad Laboratory, NTNU from January 2013 to June 2013.

The project is part of a research program carried out in collaboration with Department of Petroleum Engineering and SINTEF Petroleum, and is sponsored by Det Norske Oljeselskap, GDF SUEZ, Lundin Norge and Statoil.

I would like to thank my supervisors Professor Gisle Øye and Post. Doc. Meysam Nourani for presenting me with an interesting topic and a very dynamic project. I've learned a lot during these six months, not only theoretically, but also in ways of approaching scientific problems. I specifically credit this to Meysam Nourani who has encouraged a dynamic approach to the topic. We've had many discussions, and I would also like to thank you for presenting me with some of your own work and study.

I declare that this is an independent work according to the exam regulations of the Norwegian University of Science and Technology (NTNU).

Eivind Joo Behrens

Eivind Joo Behrens

Trondheim, 12.06.2013

Summary

Chemical flooding, or surfactant flooding, is a well known EOR technique which has been used worldwide for decades. For this method to be economically feasible, it is crucial to minimize the loss of surfactant to the reservoir. Currently the industry is considering combining chemical flooding with the newer technique of low salinity waterflooding which also has proved to be an efficient method for increasing oil recovery from reservoirs. In this study the adsorption of the anionic surfactant Aerosol OT onto kaolinite has been investigated by the indirect method of measuring surface tension.

The adsorption studies were conducted under four different salinities, categorized by ionic strength and ionic composition. The experiments were performed with and without calcium to study the effect of ionic composition. The ionic strength of the solutions were 0,6 and 0,2.

The results reveal that adsorption of Aerosol OT does occur onto kaolinite, and that reducing the ionic strength of the solution also reduces adsorption. The presence of divalent cations was found to promote adsorption.

The method which was utilized for this study was considered to have limited accuracy and thus more experiments would be preferred to confirm the results. The tendencies of adsorption are however in agreement with the theories of similar studies and should be considered to be valid.

Sammendrag

Kjemisk flømming med overflate aktive stoffer er en vel kjent metode for å øke oljeutvinning som har vært i bruk over flere tiår. En av ulempene med denne formen for utvinning er at tap av disse overflateaktive stoffene under flømmingen medfører store utgifter. Oljeindustrien vurderer for tiden å kombinere denne metoden, med injeksjon av vann med lavt saltinnhold. Injeksjon av vann med lavt saltinnhold er en nyere metode for å øke oljeutvinning. Dette prosjektet tar for seg adsorpsjon av det overflate aktive stoffet Aerosol OT på kaolinit. Forskningen ble utført ved hjelp av overflate spennings metoden.

Forskningen tok for seg vann med fire forskjellige saltinnhold som kategorisert etter ionestyrke. Forsøkene ble foretatt med og uten calcium, og med ionestyrke på 0,02 og 0,6.

Resultatene viser at Aerosol OT adsorberes på kaolinit. Trendene viser samtidig at lavere saltinnhold reduserer mengden Aerosol OT som adsorberes. Tilstedeværelse av calsium forårsaket høyere grad av adsorpsjon.

Metoden som ble benyttet under disse studiene ble ansett til å ha dårlig nøyaktighet og et større antall eksperimenter hadde vært å foretrekke. Tendensene som ble observert under forsøkene er allikevel i overensstemmelse med teorien og tidligere studier som har blitt foretatt på samme emne.

Index

1 Introduction

Many oilfields on the Norwegian continental shelf are on the verge of entering the tail production phase. At the current point in time, EOR (enhanced oil recovery) methods such as WAG (water and gas injection) has been used extensively, and several field trials report positive and successful feedback. Successful field trials include the Kuparuk, Snorrae and Gulfaks fields [1].Christensen et al. published results showing that WAG injection gives improved recovery compared to normal water injection, due to better sweep and lower residual oil saturation [2]. The understanding of the pore scale physics of WAG injection is however still incomplete.

The depletion of underground oil reservoirs has led the oil industry into thinking of new innovative methods of further increase the recovery rate of these reservoirs. Chemical flooding or surfactant flooding is a well known EOR technique that has been used worldwide for decades, whilst low salinity water flooding is a newer technique which has only been used in single well tests. The industry is currently considering a combination of low salinity water flooding and surfactant flooding to be an interesting EOR approach, as an alternative to the stand-alone techniques.

Loss of surfactants to the reservoir is however a central issue that restrains this method. Low retention of surfactants in the reservoir is crucial for the method to be efficient and economically feasible.

The aim of this project is to study the effect that, pH, salinity, and ionic composition will have on the adsorption of the anionic surfactant, Aerosol OT, onto kaolinite which is a type of clay that is found in reservoirs worldwide. This will be accomplished by an indirect method of measuring adsorption, the surface tension method, which will be further explained later on in the introduction and in Chapter 3, Materials and Methods.

The structure of the report is as follows: The introduction chapter will explain the problem clarification, from the general issues such as oil extraction, to the more specific of surfactant adsorption. Followed by this is a short explanation of enhanced or increased oil recovery methods and how this relates to the issue at hand, adsorption of surfactants onto clay materials, will be given. A short briefing of previous studies on the field, and why the indirect method of measuring adsorption has been chosen for this project will be given at the end of this chapter. A deeper theoretical understanding of the fundamentals of surfactants and how they interact is given in Chapter 2, Theoretical Background. Chapter 3, Materials and Methods includes a more detailed description of the materials that were used and how the experiments were carried out. The results of these experiments followed by a description and interpretation are presented in Chapter 4, Results and Discussion. The summary of conclusions that has been reached during the course of the project will finally be given in Chapter 5, Conclusions. Each main chapter has a short introduction that hopefully helps navigate through the chapter.

1.1 Enhanced Oil Recovery

The increasingly large energy consumption of the modern world demands higher productivity of the current energy sources which are available. Many oil fields are currently reaching the rim of their natural depletion and thus EOR projects supplies an increasing percentage of the world’s oil supply.

Essentially EOR methods can be categorized into three main categories: Gas Methods, Improved Waterflooding Methods, and Thermal Methods. Historically one can say that the gas method was the first implemented EOR technique, where about a hundred years ago, producers injected gas or air into reservoirs to increase the pressure and maintain recovery rate [3]. Thermal methods are mostly applied for reservoirs containing heavy oils and bitumen. The compositions in these reservoirs contain larger proportions of asphaltenes which makes the oil particularly viscous. Most of these reservoirs are located in the Northern or Southern part of America [4]. The waterflooding methods include; low salinity flooding and chemical flooding, it’s herein flooding of surfactants have become an increasingly interesting subject.

Basically the lifespan of an underground reservoir can be divided into three stages:

1.1.1 Primary Recovery

After the well has been established, the conventional oil recovery method usually relies on the natural mechanisms of the reservoir for extraction. The natural pressure of the reservoir will initially act as the main driving force of extraction. Mechanisms such as expansion of the natural gas at the upper levels of the reservoir, and expansion of lighter gas components primarily dissolved in the oil, help maintain the pressure. An average of 5 to 25% of OOIP

(Original oil in place) can be extracted from an underground reservoir by natural depletion [5]. This is of course highly dependable on the reservoir, both in terms of structure, sand and clay composition, temperature, pressure and also composition of the oil.

1.1.2 Secondary recovery

As the recovery rate of natural depletion decays, EOR techniques are needed to maintain productivity. The secondary stage of oil recovery involves methods which supplement the driving force of natural depletion. This can be accomplished by pumping, or the more popular choice of injecting gas, air, or water into the reservoir. A combination of water and gas, WAG (Water Alternating Gas) has proven to be highly effective. This process was originally developed with the aim of increasing the permeability in the reservoir by alternating the flow of gas and water injection to the reservoir. Figure1.1.1. shows a schematic view of the WAG process.

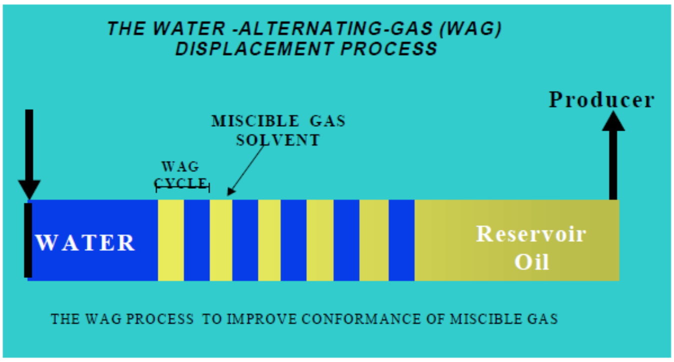

Figure 1.1.1Schematic overview of the WAG injection process [6].

Gas and water slug injections are carried out in cycles. Both fluids are injected into the well, followed by waterflooding for displacing volume. By injecting 40% of HCPV (hydrocarbon pore volume), some projects have reported increased recoveries of 9-12% [6].

Reports of WAG applications from the Statfjord field suggest that WAG may be able to increase oil recovery by up to 13 % over the production of normal waterflooding. Excellent results were also reported from the Gulfaks and Oseberg fields. At the beginning of the century the target for Norway was an increase in oil recovery from 36 to 45% OOIP using WAG processes [6].

1.1.3 Tertiary Recovery

To further increase recovery rate after the suggested WAG process, both low salinity water and chemical -flooding has been proposed as rather new technologies. The latter method is still young of age, but extensive resources have been put into research and development within this field the past few decades.

Low salinity waterflooding involves, as the name states, flooding the reservoir with low salinity water. Seawater typically has a salt content of 35 000 ppm, whilst the water used for low salinity waterflooding would normally be in the range of 500-3000 ppm. Both laboratory and field tests indicate that low salinity waterflooding contributes to increased oil recovery. Y. Zhang et al. reported significantly higher (7-14% OOIP) oil recovery by flooding reservoir cores with low salinity brines of 1 500 ppm compared to high salinity brines of 30 000 ppm[7]. Although the effect of low salinity water flood has been well known for the past decade, the mechanism behind the increase in oil recovery is still under debate. A few suggestions which have been proposed by other researchers will be given.

The pH under reservoir conditions is normally by close to 5. At this pH clay, such as kaolinite, act as a cation exchange material and thus adsorbs both protonated components of the crude oil, and cations, preferably divalent cations such as Ca^{2+} or Mg^{2+}. Tor Austad et al. proposed that the injection of a low saline fluid, which would promote desorption of the divalent cations would cause a local increase in pH close to the kaolinite surface as H^+ from the water substituted the cations. A fast reaction between OH^- and the protonated alkaline or acidic material would then cause desorption from the clay [8].

Other studies, such as those performed by Ramez A. et al. concluded that the expansion of the electrical double layer caused by low-salinity waterflooding was the dominant mechanism for improved oil recovery [9].

The other tertiary method of EOR, surfactant flooding, is the one that will be addressed in this project. The principal mechanism of surfactant flooding is to reduce the interfacial tension between water and oil, thus increasing the amount of oil recovered. Over the past few decades, a lot of attention and research has been devoted to this area. The main problem with this method is however that the economical feasibility is hindered due to loss of surfactants to the reservoir. There are a number of factors that may contribute to loss of surfactants, such as, surfactant precipitation, trapping in immobile phases, and, as the topic of this project reads, adsorption of surfactants onto rock and clay materials in the reservoir. This study will specifically focus on the adsorption of the anionic surfactant Aerosol OT onto kaolinite.

1.2 Surfactant properties

The focus of this study will be the adsorption of the anionic surfactant, Aerosol OT onto Kaolinite. Surfactants can primarily be categorized into four distinct groups, based on their polar headgroup; anionics, cationics, non-ionics, and zwitter-ionics.

Anionic surfactants generally have good surfactant properties (lowering IFT), they are relatively stable and robust, and they exhibit noticeably less adsorption onto reservoir rocks than cationic surfactants. Another important feature is of course that they can be economically manufactured. Loss of surfactants to the reservoir, either by adsorption, trapping, or other phenomena is inevitable. For surfactant flooding to be feasible, it's crucial that the surfactant can be produced economically [10].

The nonionic surfactant's ability to reduce the IFT is generally lower than for the ionic categories. They are more robust and much more tolerant of high salinity brine. Nonionics are primarily used as co-surfactants, to improve the behavior of surfactant systems [10].

Gemini surfactants

The name "Gemini Surfactants" was in 1991 given to a group of amphiphiles which had the following structure, in sequence: a hydrocarbon tail, an ionic group, a spacer, a second ionic group, and another hydrocarbon tail [11]. A schematic view of s Gemini surfactant is shown in Figure 1.2.1:

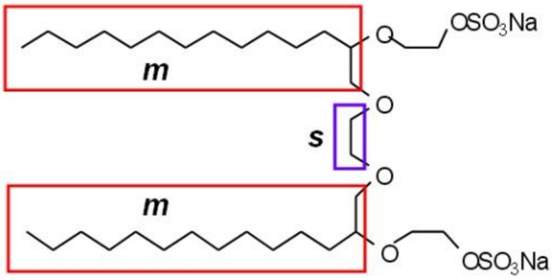

Figure 1.2.1 Schematic illustration of a gemini surfactant [12]

This group of surfactants show extraordinary robustness and perform well under high temperature and high salinity conditions [12], conditions which are typically encountered in oil reservoirs.

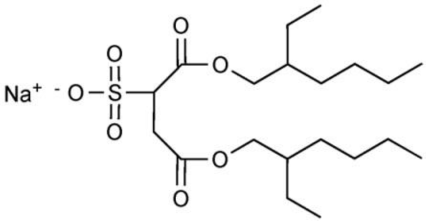

Figure 1.2.2 chemical structure of Aerosol OT [13]

Aerosol OT is an anionic Gemini surfactant which undergoes the category, sulfonated hydrocarbons, which are the most common surfactants used in micellar/polymer flooding systems. These anionic surfactants are in wide use due to the properties just mentioned, and thus it’s interesting to study their behavior [10]. Figure 1.2.2 illustrates the chemical structure of Aerosol OT.

1.3 Previous work

As enhanced oil recovery by surfactant flooding has been extensively researched over the past decades there are numerous others that have studied the main issues of the extraction method, namely adsorption of surfactants onto rock or clay in the reservoirs.

Amongst researchers who has done similar work on the field are W.Zhou et al. who studied the effect that alkali and salinity would have on surfactant adsorption on sand and oil-water interface in heavy oil/water/sand systems. In their work they applied an extraction method to determine surfactant adsorption onto sand. They concluded that addition of alkali reduced surfactant adsorption whilst, addition of an electrolyte, NaCl, increased adsorption. They also found that addition of heavy oil to the system reduced the adsorption of surfactant onto sand by 40% [14]. Although the methods applied in their studies are dissimilar to the ones used in this project, their results are highly relevant to this study.

There are numerous different ways of approaching the study of surfactant adsorption onto clay or rock materials, some of which will be mentioned in Chapter 2, Theoretical Methods. The surface tension method will be applied in this study. By this method, surfactants in solution are exposed to clay or rock material, after the assumed equilibrium of adsorption is reached, they are separated. An increase in surface tension would indicate loss of surfactant to the rock or clay material.

Mazen Ahmed Muherei and Radzuan Junin applied this method for creating equilibrium adsorption isotherms for both nonionic and anionic surfactants onto shale and sandstone [15]. Similar studies but by the use of different methods of determining surfactant concentration in solution after equilibrium have also been used. Zargham Salari et al. studied cationic surfactant adsorption onto carbonate rocks [16]. The method of conducting the experiment was the same, with one exception; they used a conductometer to determine the surfactant concentration after equilibrium.

Older similar studies of using the surface tension method for defining surfactant concentration after reached equilibrium include Wayne F. Howers investigation of adsorbance of anionic and non-ionic surfactants onto montmorillonite [17].

1.4 An indirect approach

The approach that was used for estimating the amount of surfactant that adsorbed to the kaolinite surface was the so called surface tension method. Most adsorption-studies of surfactants in dispersed systems are performed by adding surfactant to the dispersion and letting the system reach equilibrium. The suspended particles are then separated from the solution and the surfactant concentration is measured [18]. There are numerous different ways of determining the surfactant concentration, but the selected method for this project was an indirect method of measuring surface tension. The practical measurements of this technique are very simple, and this was also some of the motivation for choosing this method for the adsorption studies. It is however an indirect approach which requires some preparations and advance work. In addition, measurements at very short timescales are difficult.

By knowing how the interfacial tension changes as a function of surfactant concentration, the change in concentration can also be estimated back by directly measuring the change in interfacial tension. This of course need to be done as a pre-study by measuring the IFT under known surfactant concentrations for the various simulated conditions. The downside to using this method is thus that the interfacial tension only changes with the concentration as long as the surfactant concentration is below CMC (critical micelle concentration), and thus all conducted experiments are also limited by the CMC. A more detailed explanation of this method will be given in Chapter 3, Materials and Methods.

2 Theoretical Background

Surfactants are widely used and find a very large number of applications because of their remarkable ability to influence the properties of surfaces and interfaces. This chapter opens with a short introduction to interfacial tension. It will then describe the fundamentals of surfactants and how they interact and affect the interfacial tension between phases. Some methods of modeling surfactant adsorption will be introduced and the surface zeta potential will be explained towards the end.

2.1 Interfacial Tension

The basics.

The tension that arises between two immiscible fluids or two different phases is termed interfacial tension. The interfacial tension between a gas and a liquid can also be termed as the surface tension. An example of such a system is the air-water interface. The origin to the surface tension is attractive forces between molecules in each phase. The molecules in the bulk of a liquid, assuming that the liquid is stationary, are exposed to the same attractive forces in all three dimensions. The molecules at the surface on the other hand, only sense forces in two dimensions. This difference is the cause of surface energy and thus also the surface tension. The dimensions of the surface tension will be annotated as force per unit of length [mN/m]. The surface tension between air and different liquids varies as the intermolecular forces in each liquid changes. However, for a system composed of two immiscible liquids, the interfacial tension is dependent on the attractive forces between the molecules in each of the two liquids. If the interfacial tension between the two liquids is reduced the two liquids will become miscible. The surface tension between air and water at 25 °C and atmospheric pressure is 72,8 mN/m [19, 20].

2.1.1 Effect of Solutes on IFT

Addition of co-solutes to aqueous solutions can and will most likely affect the surface tension of a system. Three main categories of co-solutes and the result they will have on the surface tension are considered. The addition of electrolytes will under most circumstances increase the surface tension as the concentration is increased. This is caused by a negative adsorption of ions at the liquid-air interface. Addition water-soluble organic compounds such as ethanol on the other hand, would likely decrease the surface tension. At last but not least the addition of surfactants will greatly decrease the surface tension. The effect of these three co-solutes is schematically shown in Figure 2.1.1.

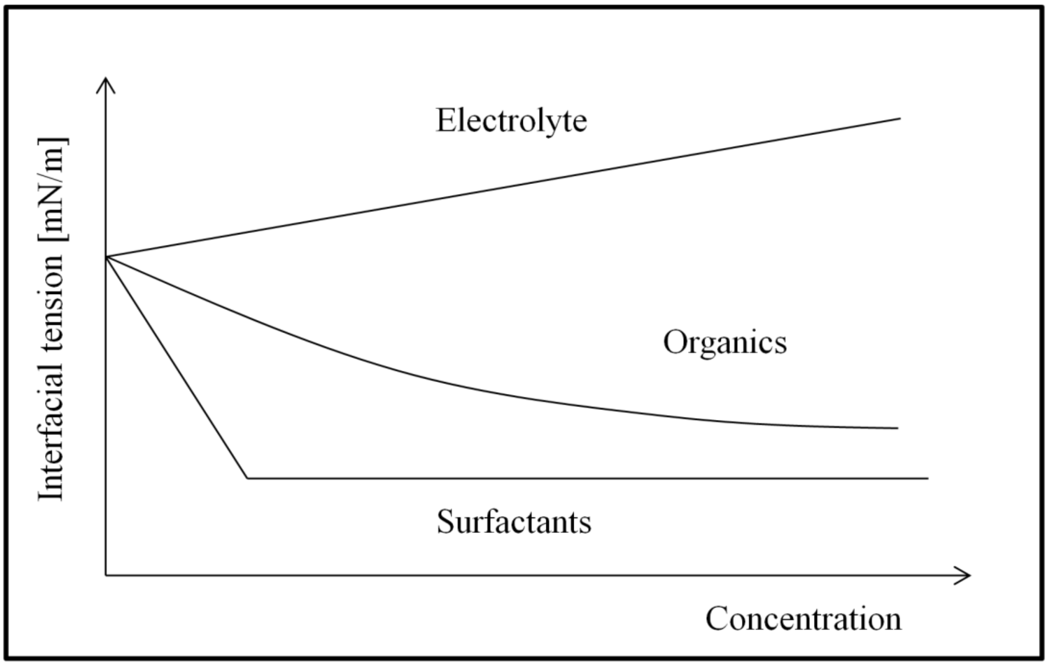

Figure 2.1.1Schematic illustration of the addition of co-solutes to an aqueous solution [21].

The effect of added surfactants shows a specific breakpoint where increasing the surfactant concentration shows no further effect on the surface tension. This phenomenon is known as the CMC (Critical Micelle Concentration) and will be described in Chapter 2.3 CMC.

2.1.2 Diffusion; changes IFT over time

The interfacial tension of a spontaneously formed interface of air and an aqueous solution may slowly change over time. This change interfacial tension is caused by rearrangements of molecules in the bulk solution. Immediately after the interface is formed, the molecular composition at the interface represents the composition in the bulk solution. Over time however, the interfacial tension will slowly decrease until it stabilizes at a constant level. This change is caused by rearrangements of the molecules in the bulk solution. Molecules and components which will lower the interfacial tension will preferably adsorb at the interface and lower the interfacial tension. The system will always try to arrange itself in a manner that lowers the interfacial tension. This is schematically illustrated by figure 2.1.2.

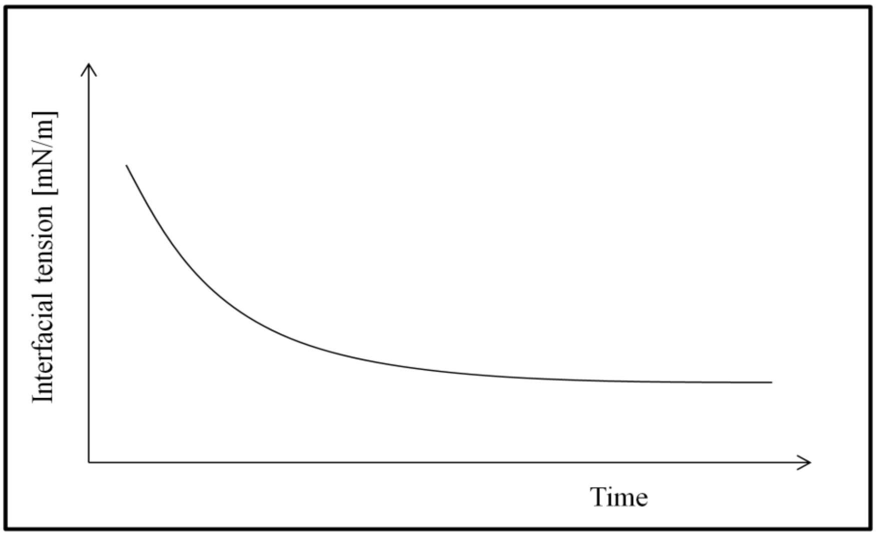

Figure 2.1.2 Schematic illustration of how interfacial tension of an aqueous solution and air can change over time

As illustrated by figure 2.1.2, the process of rearrangement and diffusion of components from the bulk solution to the interface is a time-dependant process. This effect is present whether the components are organics or surfactants but the timeframe varies.

2.2 Surfactants

Surfactants are surface active compounds; this means that they have a tendency to adsorb at interfaces. The driving force of surfactant adsorption is to lower the free energy of the interface, more commonly known as the interfacial tension. Interfacial tension is measured as force per unit of length, or energy per unit of area. By this definition the interfacial tension between two immiscible phases is equivalent to the amount of work required to expand the interface. As mentioned the driving force of surfactant adsorption at interfaces is to lower the interfacial tension. A tighter packing of surfactants at the interface will further reduce the interfacial tension.

The molecular structure of surfactants consists of two parts, a hydrophilic head group and a hydrophobic tail. It’s the combination of these parts that gives the surfactant its unique properties and ability to reduce interfacial tension. Figure 2.2.1 illustrates a schematic illustration of a surfactant:

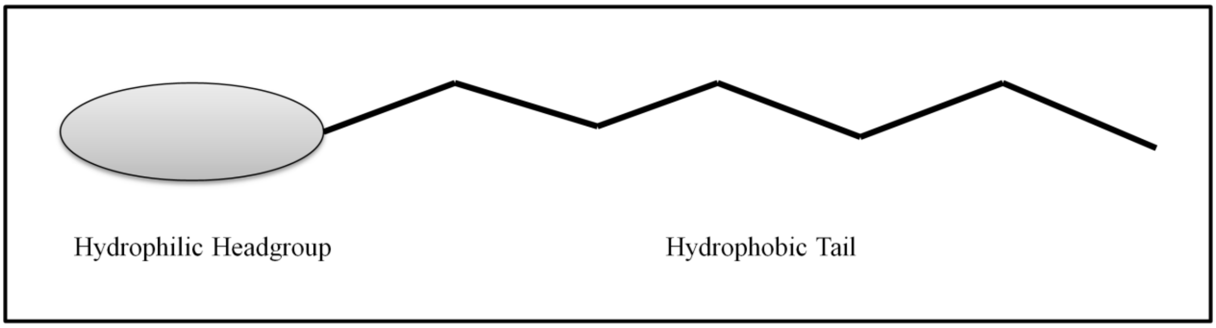

Figure 2.2.1 schematic illustration of surfactant

Surfactants in aqueous solutions which adsorbs at a hydrophobic surface will normally adsorb to the interface with the hydrophobic tail attached to the hydrophobic surface and the hydrophilic head group presented towards the aqueous solution. With this arrangement the hydrophobic surface will become hydrophilic and thus reduce the interfacial tension[21].

As surfactants are used to reduce the interfacial tension between two phases, the degree of how good a surfactant is should be dependent on its tendency to adsorb at the interface. Basically this means that the stronger tendency, the better the surfactant. Since the affinity of a surfactant towards an interface is dependent on both the type of surfactant and also the nature of both phases that compose the interface, there is no universally good or best surfactant. Due to this fact there are a large variety of different surfactants and they can be classified by their polar headgroup; cationics, anionics, non-ionics and zwitterionics. As mentioned in the introduction, Aerosol OT, which is the surfactant used for the studies of this project is classified as an anionic surfactant.

2.3 Critical Micelle Concentration

Under low concentrations, surfactants in aqueous solutions behave similarly to electrolytes. If the concentration is increased however, the behavior will alter quite a lot from the common electrolyte. By increasing the surfactant concentration in bulk solution, the amount which accumulates at the interface will increase and further lower the interfacial tension. There is however a limit to the amount of surfactants that can accumulate at a given area of interface. Under normal circumstances that limit is reached when the surfactants start to aggregate and form micelles in the bulk solution [22]. This concentration is known as the critical micelle concentration, hereby referred to as the CMC. The formation of micelles is a mechanism for surfactants to reduce the exposure of their hydrophobic tail to the aqueous solution. The CMC is the concentration of maximum solubility of a monomer in a particular solvent [23]. This phenomenon is very important because it alters the properties of the micellized surfactants. Only surfactant unimers contribute to lowering of the interfacial tension. This means that increasing the surfactant concentration above CMC will have no effect on the surface or interfacial tension. This is illustrated on figure 2.3.1:

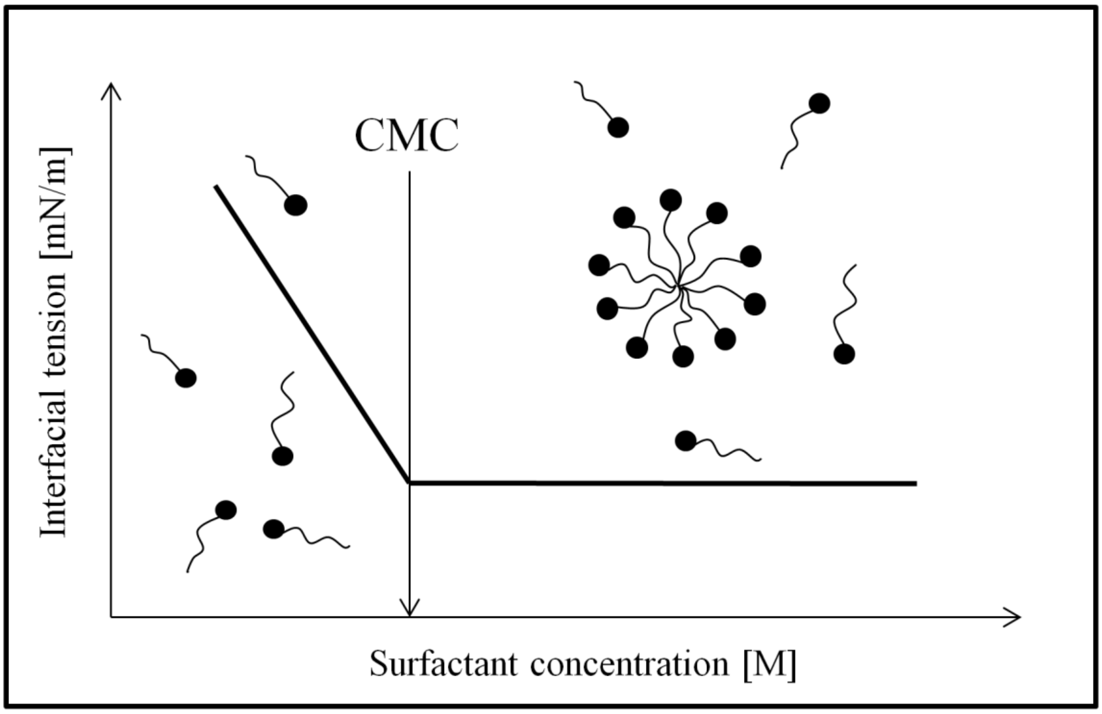

Figure 2.3.1 Schematic illustration of CMC

Chemical structure of surfactant affects the CMC

The chemical structure of the surfactant is one of the parameters that determine the CMC. This applies to the size and shape of the head of the surfactant, and also the tail. A list of physical parameters of the surfactant that determine the CMC is given below [24]:

- Increasing the chain length of the tail will strongly decrease the CMC. A general rule of thumb is that the CMC decreases by a factor of 2 per methylene group that is added to the tail for the ionics, and even stronger, by a factor of 3 for non-ionics.
- The CMC of ionic surfactants are much higher than for the non-ionics.
- For ionic surfactants the nature of the headgroup doesn’t affect the CMC drastically, although cationics generally have a higher CMC than anionics.
- For non-ionics the CMC increases moderately as the head group becomes larger.
- Increasing valency of the counterion will drastically reduce the CMC. Organic counterions reduce the CMC compared to inorganic counterions.

- Perfluorination of the alkyl chain lowers the CMC; however partial fluorination may actually increase the CMC. This is credited to the unfavorable interactions between hydrocarbon and fluorocarbon groups.

Other parameters that affect the CMC

Temperature will influence the CMC in a lesser manner. Over a temperature range from roughly 10 to 50 °C, the CMC for the common non-ionic and ionic surfactants changes by less than 20 percent. Also, pressure has little influence on the CMC, even up to high values [24]. The effect of added electrolyte is however significant on the CMC of ionic surfactants, and also a topic which is very central for this project. A list of the effects caused by addition of an electrolyte is listed below:

- Addition of salt/electrolyte drastically decreases the CMC. This tendency is enhanced as the chain-length of the surfactant is increased.
- As a result the CMC is much more sensitive to change in chain-length at higher salt concentrations than lower concentrations.
- The effect of added electrolyte depends strongly of the valence of the ions. It is most sensitive to the valence of added counter-ions.
- The noted observations added electrolyte to non-ionic surfactant systems are very small compared to that of ionic systems.

Surfactant Solubility; Related to the CMC

Although temperature has little effect on the CMC, it has a great impact on the solubility of surfactant systems. As the temperature rises, the solubility of surfactants is increased. A noteworthy phenomenon which relates the solubility to the CMC is registered as the temperature is increased. At a certain temperature the solubility as a function of elevated temperature increases drastically. This point is known as the Kraft point, and it’s a phenomenon that occurs as the solubility curve crosses the CMC curve. This is schematically illustrated in figure 2.3.2:

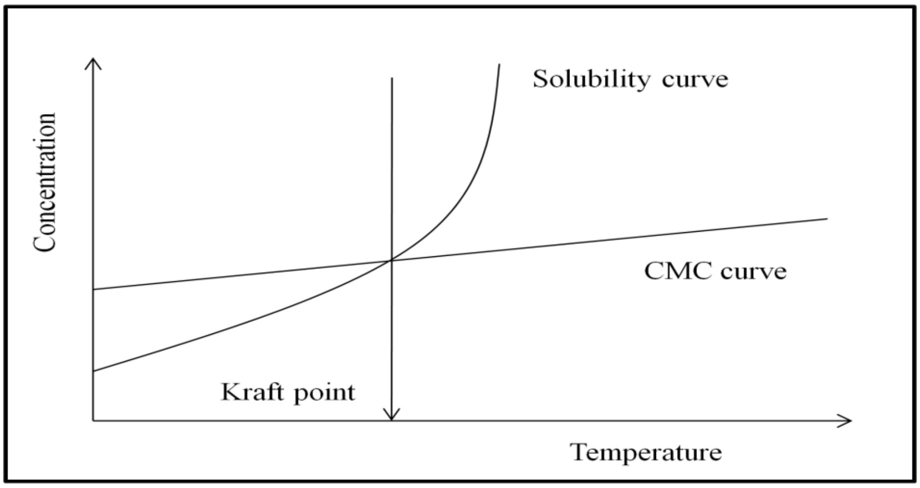

Figure 2.3.2 Schematic illustration of the Kraft point

The Kraft phenomenon is explained by the formation of micelles as the solubility curve crosses the CMC curve. At concentration below CMC, the solubility is purely limited by the unimers solubility. As the solubility curve crosses the CMC curve the amount of surfactants added can be increased while the numbers of free unimers in solution remains more or less the same. The excess amounts of surfactants form micelles and thus the amount of free unimers in solution remains constant [24].

Methods of measuring CMC

There are numerous different ways to measure the CMC of a surfactant. An obvious choice from the description in Chapter 2.1 Interfacial Tension would be to measure and plot the interfacial tension for various concentrations of the surfactant. Other methods include measurements of solubility, self-diffusion measurements, nuclear magnetic resonance (NMR), or fluorescence spectroscopy. By obtaining the CMC for a surfactant from several of these methods, the results would naturally deviate somewhat from each other. The CMC can thus be considered to be a range of concentrations instead of just one exact point of concentration. For the long-chained amphiphiles with strong association to each other this range is shortened and the results of the various methods of determining the CMC yields very similar results. However, for the short-chained, more weakly associating amphiphiles the results from the different measuring techniques might vary more [24].

2.4 Critical Packing Parameter

When micelles form in aqueous solutions, the surfactants tend to arrange with their hydrophilic tail directed towards the aqueous solution, and their hydrophobic tail stacked together to minimize exposure. The most intuitive and simplest geometrical formation of such a micelle is a spherical formation such as illustrated in Figure 2.4.1.

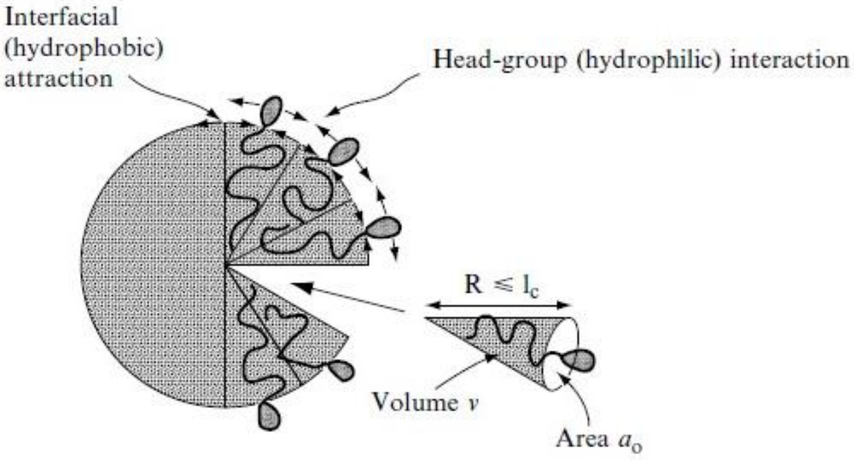

Figure 2.4.1 Illustration of micellar structure [19].

One way of describing the micelle structure is done through the CPP (Critical Packing Parameter). The derivation of the CPP for a spherical micelle is given below:

Derivation of CPP for a spherical micelle:

The number of surfactants clustered in a micelle can be expressed as the aggregation number, the ratio between the volume of a micelle and the volume of a single surfactant. This is illustrated by the following equation [25]:

$$N = \frac{V_{micelle}}{v} = \frac{\frac{4}{3} * \pi * R_{micelle}^3}{v}$$

Where N is the aggregation number, $V_{micelle}$, is the total volume of the micelle, v is the volume of one chain, and $R_{micelle}$ is the radius of the micelle, which equals the length of a chain. The aggregation number can alternatively be expressed as the ratio between the micellar area and the area of one surfactant molecule as follows:

$$N = \frac{A_{micelle}}{a} = \frac{4 * \pi * R_{micelle}^2}{a}$$

Where $A_{micelle}$ is the area of the micelle, and a is the area of one surfactant molecule. Merging these equations will result in:

$$\frac{v}{(R_{micelle} \; * a)} = \frac{1}{3}$$

This is known as the CPP for a spherical micelle. The definition of the CPP is thus the ratio between the tail volume and the radius of the micelle multiplied with the area of the headgroup. If however the surfactant has a tail which is twice as long or even two tails, such as AOT, other geometrical arrangements would be favored. Figure 2.4.2 illustrates a few other geometrical shapes of micelles and their corresponding CPP.

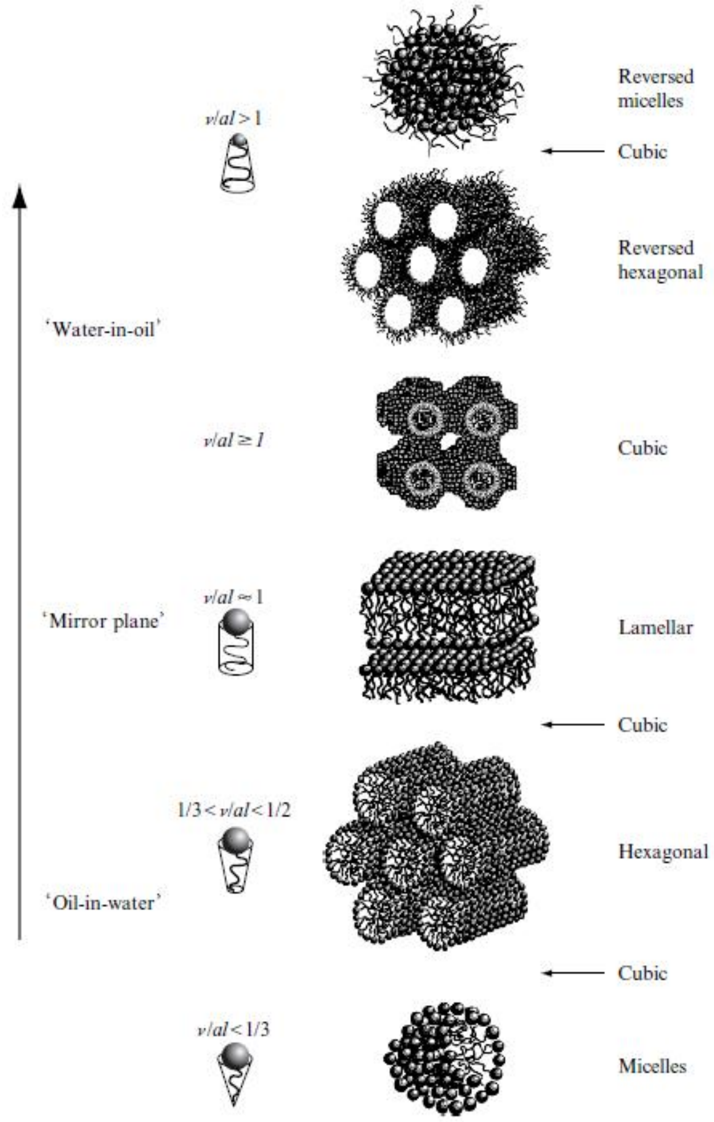

Figure 2.4.2 illustration of different structures of micelles [19, 26].

Surfactant Adsorption at Liquid-Air Interface; Related to the CPP

Surfactants adsorb at the air-water interface with their polar headgroup arranged towards the water phase and their hydrophobic tail extended towards the air. When an electrolyte is added to the surfactant solution, a number of effects take place; the CMC decreases, the interfacial tension above CMC decreases, and the slope of the curve just below CMC increase, which again indicates a higher surfactant adsorption at the interface[19]. These observations indicates a higher CPP, ergo the surfactants pack more tightly. This effect is credited to the electrolyte's ability to shield the repulsive headgroups of the surfactants[19].

2.5 Adsorption at the interface

The definition of the surface of air-liquid system with a solute was first made by Gibbs. He defined it to be the position where the solvent concentration is half between that in the solvent and in the vapor. Surfactants that adsorb at the surface provide an expanding force which acts against the normal surface tension and lowers it. For non-ionic surfactants the relationship between the surface tension and surfactant adsorption is given by the equation [19, 27]:

$$\Gamma = -\frac{1}{\mathrm{RT}}\frac{\mathrm{d}\gamma}{\mathrm{dln}\ a}$$

Where Γ is the adsorption of surfactants at the interface, γ is the interfacial tension, and a is the activity of solute in bulk solution. At very low concentrations the surfactant activity can be replaced by surfactant concentration, *C*, which yields:

$$\Gamma = -\frac{1}{\mathrm{RT}}\frac{\mathrm{d}\gamma}{\mathrm{dln}\ C}$$

For ionic surfactants without the presence of an electrolyte there is a counterion coupled with the surfactant since the surface as a whole needs to be electrically neutral. The equation is then rewritten:

$$\Gamma = -\frac{1}{2\mathrm{RT}}\frac{\mathrm{d}\gamma}{\mathrm{dln}\ c}$$

If however an electrolyte is present in the solution, one of the first two equations should be applied as the electrolyte “shields” the effect of the counter-ion and each surfactant adsorbs as a single species.

2.6 Adsorption on solid surfaces

As mentioned in Chapter 2.2 Surfactants, the adsorption of surfactants to an interface is dependent on the interaction of the surfactant with the surface. For surfactants in an aqueous solution, adsorption is also determined by the hydrophobicity of the surfactant. The latter has been found to be the dominating driving force of adsorption for many scenarios. Examples of this are displayed for adsorption onto hydrophobic surfaces where the surfactant adsorbs with their hydrophobic tail to the surface, and the hydrophilic headgroup exposed to the solution.

The other scenario is shown for very polar surfaces where surfactants adsorb with their headgroup towards the surface and their hydrophobic tail towards the solution. Since it's unfavorable to have their hydrophobic tail exposed to the aqueous solution, these systems tend to form double layers if the concentration of surfactants allow for it. Schematic illustrations of different configurations of surfactant adsorption are shown in figure 2.5.1 [28].

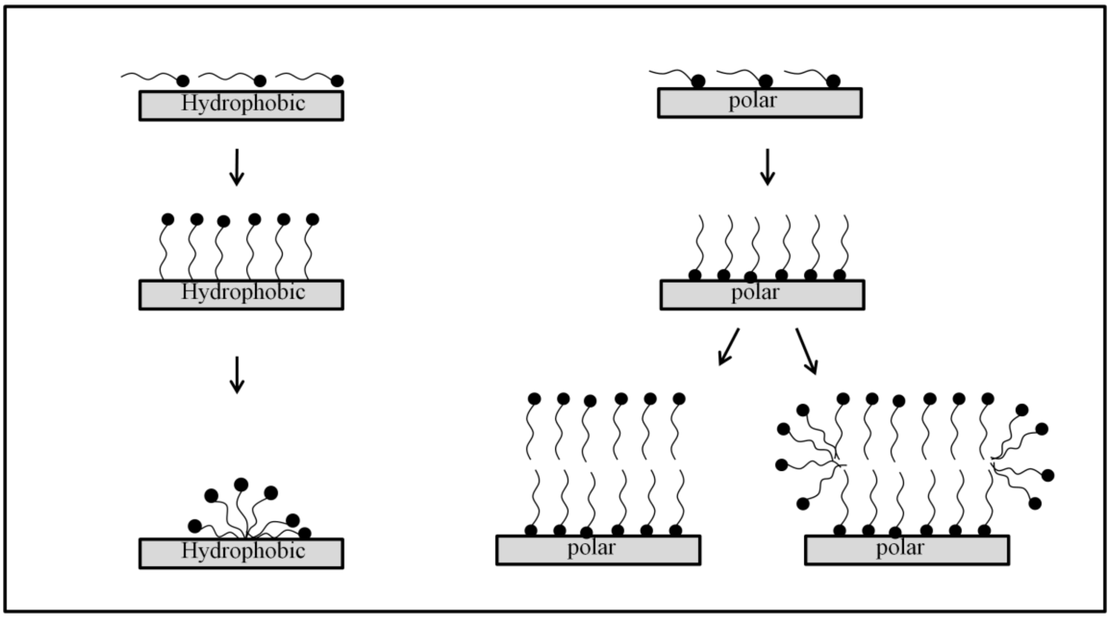

Figure 2.5.1 illustration of surfactants adsorbed to polar and hydrophobic surfaces [28].

If the attraction between the headgroup and the surface is intermediate in strength, aggregates or micelles may form at the interface. This will occur when the hydrophobic attraction of the tail parts of the surfactant exceeds the strength of interaction between the headgroup and the interface. Aggregation of surfactants at the interface is thus a matter of balance between these two forces. A parameter that reflects both of these forces is the CPP. The CPP is therefore a relevant factor considering surfactant adsorption. Adsorption increases as the CPP is increased. A list of parameters which increase the CPP of a system containing a single straight-chained ionic surfactant follows [18]:

- Increasing the chainlength of the tail
- Increasing the branches of the tail
- Use of surfactants with two tails
- Addition of a hydrophobic amphiphilic molecule
- Addition of hydrophobic non-ionic surfactant
- Addition of small amounts of surfactant with opposite charge.
- Addition of electrolyte

A list of parameters that will increase the CPP for a single straight-chained non-ionic surfactant follows:

- Increase the chainlength of the tail
- Increasing the branches of the tail
- Use of surfactants with two tails
- Use of surfactant with a smaller headgroup; shorter polyoxyethylene chain.
- Increase temperature
- Addition of electrolyte.
- Addition of ionic surfactant

Adsorption of ionic surfactants to hydrophilic surfaces.

Adsorption of ionic surfactants to a hydrophilic surface is almost exclusively driven by the ion-exchange mechanism if the concentration is very low. When this mechanism takes place, counterions in the diffusive double layer are exchanged for surfactants with the same charge. This leads to a higher concentration of surfactant close to the surface. This mechanism can thus induce micellization close to the interface even if the bulk concentration is below CMC. The arrangement and shape of these micelles are still being debated. There is however a general agreement that aggregation of surfactants does happen at the surface. At higher concentrations it’s believed that the surfactants will form a double layer.

2.7 Effect of impurities on interfacial tension data

Krister Holmberg et. al. commented on the effect of impurities on surface tension data. For surface tension measurements of sodium dodecyl sulfate (SDS) as a function of surfactant concentration [19]. They noted a minimum in surface tension which they credited to the formation of dodecyl alcohol by hydrolysis of SDS molecules. Since dodecyl alcohol is more surface active than SDS this would cause a minimum in surface tension. However, as the concentration was increased and micelles were formed, the dodecyl alcohol would be solubilized in the micelles and thus be desorbed from the interface. As a result, the surface tension would then increase. They concluded that whenever a minimum was found in a surface tension versus surfactant concentration plot, the sample contained impurities that are more surface active than the original surfactant.

From this experiment they observed that the surface tension may decrease slowly for a very long time before equilibrium is obtained. This could be the cause of very low concentrations of impurities, and also that diffusion from bulk to the surface was the rate determining factor. From this they noted that the ratio between surface and volume of the bulk could affect the results of the interfacial tension data. A larger bulk volume per area of interface would allow for more impurities.

2.8 Models and methods to determine adsorption

Determining surfactant adsorption in dispersed systems is almost exclusively done by adding a known amount of surfactant to the system, waiting for the system to reach equilibrium, separating the dispersed solids, followed by measuring the surfactant concentration in the solution. Surfactant adsorption is then given by the following equation:

$$\Gamma = \frac{(C_0 - C)V}{m a_{sp}}$$

Where Γ is the amount adsorbed [mg/m^2], C is surfactant concentration in solution after equilibrium is reached [mg/ml], C_0 is the initial surfactant concentration [mg/ml], V is the volume of solution [ml], m is the mass of particles [g], and a_{sp} is the specific area of the particles. Various ways of determining the surfactant concentration in the solution after separation include; ion-selective electrodes, UV/vis spectroscopy, refractive index, titration, chromatography or surface tension. For this project the latter method has been applied. For use of this method, separation of particles from the solution isn't needed, provided that the particles are completely wetted by the liquid as they won't affect the interfacial tension [18].

2.8.1 Langmuir Adsorption isotherm

The Langmuir isotherm is often used as a theoretical model for analysis of adsorption onto surfaces. For appliance of the Langmuir equation, the following assumptions have been made [29]:

1) The surface is homogeneous
2) Surfactants may only adsorb in one monolayer
3) There are no surfacatant-solvent or surfactant-surfactant interaction

4) The surfactant and solvent molecules have equal cross-sectional surface areas.

The first two assumptions are considered to be quite reasonable, with the exception shown in Chapter 2.6 Surfactant Adsorption onto Solid Surfaces, that surfactants may form double layers at the interface. The latter two assumptions however are less in coherence with surfactant adsorption theory. It has however been shown empirically that they deviate in opposite directions and more or less cancel each other out and thus the Langmuir equation may still show quite good similarities when modeling surfactant adsorption. The Langmuir equation can be derived as follows [29]:

The rate of adsorption can be defined as:

$$\text{Rate of } adsorption = \ k_a C(1 - \mathbf{\Theta})$$

Where C is the surfactant concentration at equilibrium, $\mathbf{\Theta}$ is the fraction of surface covered with surfactants, and k_a is a rate of adsorption constant. Same as the rate of adsorption, the rate of desorption can be defined as:

$$\text{Rate of } desorption = \ k_d \mathbf{\Theta}$$

Where k_d is the rate of desorption constant. At equilibrium the rate of adsorption will be equal to the rate of desorption and the following equation is derived:

$$\mathbf{\Theta} = \frac{KC}{1 + KC}$$

Where K is the newly defined equilibrium constant [k_a/ k_d].

Nonionic surfactant systems with low concentration can be considered to follow the Langmuir type adsorption isotherms on charged surfaces. For higher concentrations the risk of forming bi-layers, disagree with the second assumption of the Langmuir isotherm [30]

2.8.2 Adsorption isotherm; Mechanism of surfactant adsorption

Based on the theories presented in the previous chapter, a common way of presenting the results of adsorption studies is to plot them as isotherms in a diagram of; amount of surfactant adsorbed per amount of adsorbent vs. surfactant concentration. These plots are often plotted in the log-log scale, but linear-log or linear-linear plots are also applicable. Abrupt changes in the slope can often be spotted in these adsorption isotherms if plotted over a wide range of concentration. How many regions of different slope-numbers depend on the concentration range and mechanism of adsorption. This again is dependent of type of surfactant, surface charge and presence or absence of other compounds. A schematic illustration of a typical four region isotherm for a monoisomeric anionic surfactant is shown in Figure 2.8.1 [31].

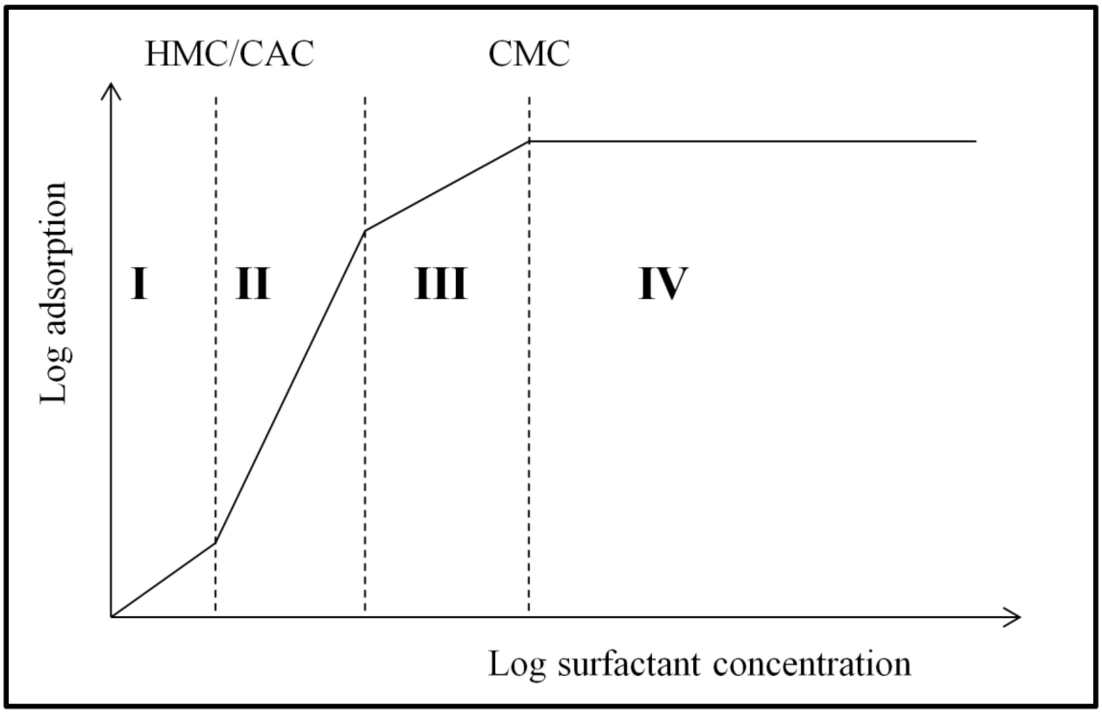

Figure 2.8.1 Schematic illustration of a typical four region isotherm.

The mechanism of adsorption in the different regions is still under discussion with more agreement for some regions than others. A proposal of mechanisms for the different regions follows:

I:

At very low surfactant concentrations the behavior of adsorption is in line with the third criteria of Langmuir’s adsorption isotherm. The surfactant molecules adsorb as individual unimers with no interaction between adsorbed molecules. The driving force and surface-surfactant interaction depends on the surface and type of surfactant. For non-ionics the interaction involves hydrogen bonding between the surface and headgroup. In addition, the hydrophobic interaction of the tail and the surface contributes to adsorption. For ionics the driving force is electrostatic interactions between the headgroups and charged sites at the surface.

II:

If the adsorption in the first region of the isotherm is driven by a mechanism where the surfactant molecules don’t interact, the second region of the isotherm will necessarily be at the concentration where there is interaction between surfactant molecules. The break between the first and second region can be referred to as the hemimicelle concentration (HMC) or the critical admicelle concentration (CAC). This would be the concentration where the first aggregate of surfactants form at the surface. The HMC or CAC varies in the same manner as the CMC. Increasing the chain length of the surfactant tail will greatly reduce the HMC/CAC. The same happens if an electrolyte is added to the system that contains ionic surfactants. A list of parameters that affect the CMC was given in Chapter 2.3, Critical Micelle Concentration. A proposed theory for why this region has a higher slope number than the first region is that the hydrophobic tail-tail interaction promotes adsorption.

III:

There are several theories describing the mechanism of adsorption in the third region of the isotherm. The decrease in slope number has been described by Somasundaran et al. as cited by Laurier L. Schramm to be a result of having filled the surface. The adsorption in the third region would then be a second layer of surfactants, where the driving force for adsorption was association of the hydrocarbon chains if the tails. It was also attributed to a reversal in surface charge as ionic surfactants adsorbed to the interface. Other theories presented by Scmaehorn et al. as cited by Laurier L. Schramm were based on the theory that a bi-layer was formed already in the second region and extended into the third region but at a different rate. The difference in adsorption would then be caused by the lack of energetically feasible sites at the surface as it’s gradually saturated.

IV:

The fourth region of the isotherm is where the CMC has been reached and no further adsorption is considered to take place. After the CMC, any added surfactant will rather form micelles than adsorb at the interface. The occurrence of this region can still happened even without a completed bi-layer of surfactants. It’s a function of a halt in adsorption and is therefore dependent on surface charge, and therefore also pH.

2.9 Zeta Potential

The net charge at a particle surface affects the ionic charge of the region surrounding the surface of the particle. Ions of the opposite charge, known as counter-ions attach at the surface of the particle. The concentration of counter-ions decrease as the distance from the surface of the particle is increased. This field of charged layers is called the electrical double layer.

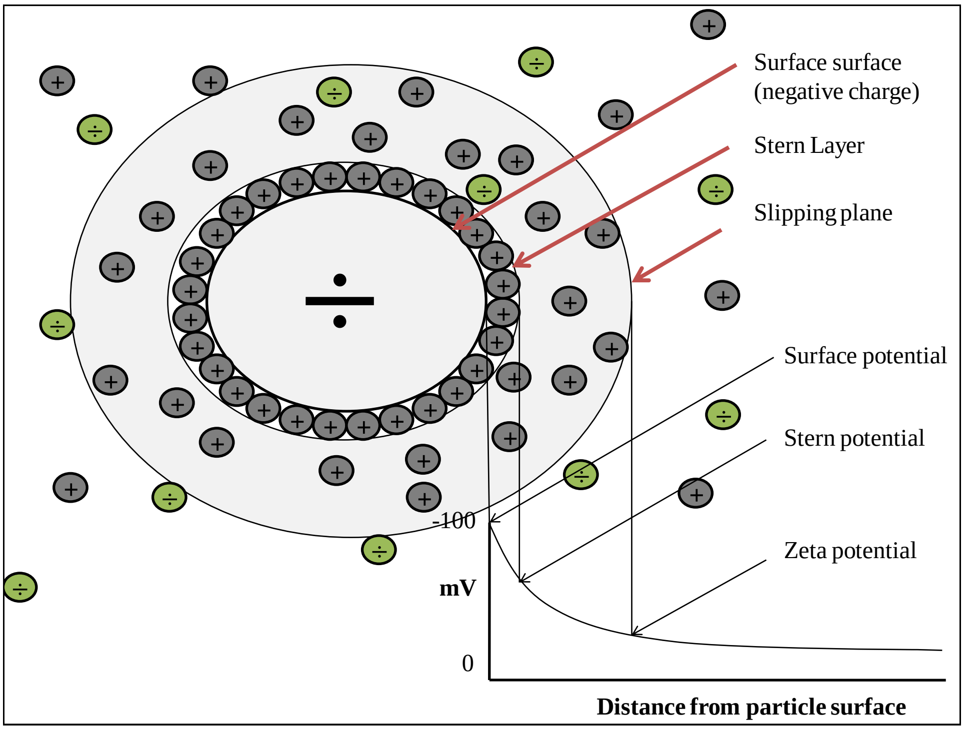

Figure 2.9.1 Schematic illustration of the double layer

The electrical double layer which is illustrated in Figure 2.9.1 is composed of two parts. One inner layer, also referred to as the Stern Layer, and the outer layer, which is often referred to as the diffusive layer. The theory concerning the electrical double layer includes; the distribution of ions close to the surface of the particle, the effect of electrolyte concentration, and how the magnitude of electrokinetic potential varies with the distance from the surface of the particle.

The Stern Layer is composed of the surface and charge of the particle, and includes potentially adsorbed molecules, such as surfactants. Here the ions are strongly bound. In the outer diffusive layer the ions are more loosely attached to the particle. In aqueous solutions these ions can have their origin from H_3O^+ and OH^-, a product of the water, or from added electrolytes. The former can usually be neglected if the solution contains an electrolyte.

As the particle moves in solution, the ions within the electrical boundary of the double layer move with it. The ions beyond the boundary stay with the bulk dispersant. The potential at this boundary is known as the zeta potential.

The zeta potential can be used to identify the colloidal stability of a system. As an example: A suspension only containing particles with a strongly negative or positive zeta potential would likely be stable due to the repellant force between particles. If the magnitude of zeta potential is lowered however, the repellant force will be reduced and the particles would be more acceptable for flocculation. As a “rule of thumb”, a dispersion which has a zeta potential with a magnitude of 30 mV or higher is under normal circumstances considered to be stable. However, if the particle density deviates from the dispersant, they will sediment [32, 33].

pH affects zetapotential

The pH is the most important factor that affects the zeta potential of a system. Without knowing the pH, the zeta potential is for all practical purposes a meaningless number. The zeta potential can be manipulated by adding either an acid or alkali to the suspension. If alkali is added to a system with a negative zeta potential, the magnitude of negative zeta potential will be enhanced. If on the other hand an acid is added, the magnitude of zeta potential will be lowered, until eventually it becomes neutralized. Further addition of acid will cause a positive charge of zeta potential.

Thickness of electrical double layer

The thickness of the electrical double layer is dependent on the concentration of ions in the solution. The ionic strength of the medium is used for calculating the thickness of the double layer since the valence of the ions in solution also affects the thickness. Increasing the ionic strength of the solution decreases the layer thickness. Increasing the salt concentration in solution will thus compress the layer.

3 Materials and Methods

A short introduction to how the experiments were carried out was already given in the introduction chapter. This chapter includes a more detailed description of the basic principles of how the surface tension method works for calculating surfactant concentration in aqueous solutions. The procedure of how the experiments were executed and how the parameters were varied will then be given. A short description of the materials and apparatus that were used will sum up the chapter.

3.1 Method

A few methods of studying adsorption of surfactants onto various materials were briefly mentioned in chapter 2.8 Models and methods to determine adsorption. The surface tension method is an indirect approach to the study of surfactant adsorption. The simplicity of measurements used for this approach is one of the main reasons it was chosen.

Basic Principle

The basic principle of this method is to determine the surfactant concentration in a solution by measuring the interfacial tension. This can be achieved by plotting the interfacial tension of a surfactant solution as a function of surfactant concentration. The surfactant concentration of a sample can then be indirectly determined by the use of this plot. If adsorption takes place the surfactant concentration in solution will decrease and the interfacial tension will increase. This is illustrated in Figure 3.1.1:

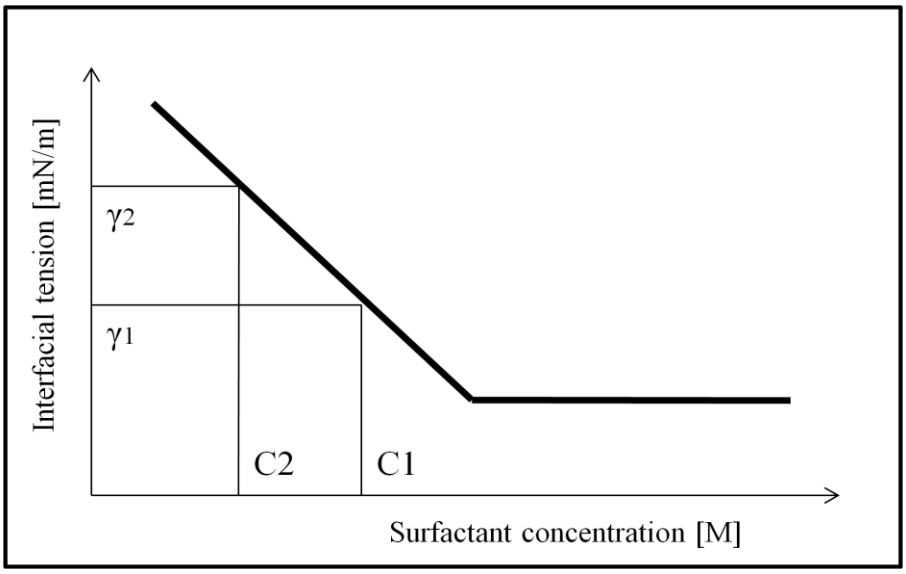

Figure 3.1.1 Illustration of how the interfacial tension changes with the surfactant concentration below CMC.

The surfactant concentration at state 1 (C1) should obviously be known even without interfacial tension measurements. However measurements could prove to be useful in determining accuracy of this method. As shown in Figure 3.1.1, if the interfacial tension measured at the second state (γ2) is higher than at the first state (γ1), this would be an indication that the surfactant concentration decreased, hence surfactant adsorption has taken place.

3.2 Procedure

As previously explained in chapter 2.3, Critical Micelle Concentration, and further illustrated in Figure 3.1.1, the surface tension is only dependent on surfactant concentration at concentrations below CMC. This means that all conducted experiments would have to be below the CMC. The practical description of the experimental procedure is given below.

Determining CMC

The first step of the procedure was to determine the CMC for the surfactant under each of the conditions that were planned prior to the experiments. The CMC is very sensitive to the electrolyte concentration and thus the CMC was determined for each of the salinities that were selected. How the interfacial tension varied with the surfactant concentration was just as important to determine. This was done by plotting the IFT as a function of concentration below CMC. Microsoft excel was then used to calculate a mathematical equation which described the relationship.

The salinities of the solutions were characterized by ionic strength. Two ionic strengths were chosen, 0,6 and 0,02. Since it was desirable to see the effect of divalent cations, two different compositions of salt was selected for each of the ionic strengths, one with purely monovalent NaCl, and one with a mixture of NaCl and $CaCl_2$. The ratio between NaCl and $CaCl_2$ in the samples with calcium was 1:45. Added up, this gave four different salinity solutions, all of which had different CMCs that had to be determined. A complete overview of the different electrolyte compositions of the samples are given in Table 3.3.1.

Preparation of samples:

The next step was preparation of surfactant solutions with different salinities. Surfactant solutions and salt solutions were prepared separately with double concentration of experimental values and then mixed fifty-fifty prior to adding kaolinite. Example: If the experimental value for a batch should have ionic strength of 0,6 and surfactant concentration of 10^{-5} Mol, a fifty-fifty mixture of $2* 10^{-5}$ Molar surfactant solution, and salt solution with ionic strength of 1,2 was used. Calculations for the different salinities are given in appendix H.

Two methods:

At this stage the procedure was split into two parallel methods of preparing the samples:

In the first method, five different surfactant concentrations were selected for each of the salinities that had been determined beforehand. For each of these concentrations, six parallel batches of surfactant solution with added kaolinite were made. An additional sample without added kaolinite was also made as a reference value to measure IFT without adsorption. The batches were stored in 50 ml centrifuge tubes of the model HP flat cap delivered by VWR. Each batch had a volume of 30 ml surfactant solution mixed with 0,3 gram of kaolinite.

The samples were shaken at 300 SPM (shakes per minute) for six individual (also pre-selected) time intervals before they were instantaneously separated by centrifuging. The time of adsorption was therefore very exact using this method. After centrifuging the surfactant solution was decantated and stored in glass vials. The kaolinite was disposed.

In the second method the samples were prepared in the glass beakers which were used when measuring the IFT of the samples with the tensiometer. The idea behind this method was to limit the sample's exposure to contamination by only using one container. The volume of solution was 30 ml mixed with 0,3 ml kaolinite, same as for the first method. The samples were shaken for 3 hours at 300 SPM and then left to sediment. The IFT was measured before adding kaolinite in addition to the different intervals which were decided upon beforehand. The disadvantage of using this method was the slow and undetermined process of separation. The separation of kaolinite from solution was done by sedimentation and this the exact time of equilibrium was hard to determine.

For both methods, the IFT was measured both prior to adding kaolinite and then again after separation.

Converting IFT measurements to concentration measurements.

The concentration of surfactants in solution was then calculated by the use of the CMC plots. The equations describing the function of each plot are given in appendix B-G.

In addition to the indirect adsorption studies using the surface tension method, measurements of the surface zeta potential of the kaolinite were also preformed. These measurements were added to help analyze and determine if surfactant adsorption onto the kaolinite really transpired.

3.3 Parameters.

Limits of the parameters were quite diffuse prior to the experimental part of the project. A study of similar projects and reservoir conditions was therefore conducted before determining the limits of parameters for the project. The type of clay and surfactant was decided upon prior to project start.

Salinity:

Most literature studies report that low salinity flooding enhances oil recovery of the reservoir. For low salinity flooding, the salt concentrations would be in the range of 500 to 3000 ppm [8]. This was therefore a natural starting point of salt-concentration. It was decided that the adsorption studies should be conducted under two different salinities. The salinity of seawater, which is approximately 35 000 ppm was selected as the other.

It was also desirable to study the effect of monovalent electrolyte compared to divalent electrolyte. $CaCl_2$ was used in addition to NaCl to provide a divalent electrolyte in the salt solution. The ratio between NaCl and $CaCl_2$ was 45:1. The samples were therefore split into four main categories; Low salinity without calcium, Low salinity with calcium, High salinity without calcium and High salinity with calcium. The concentration was determined by Ionic strength. The Ionic strength was 0,6 for the high salinity samples and 0,02 for the low salinity samples. A table showing the salt composition of the four main categories is given in Table 3.3.1:

Table 3.3.1 Overview of the different electrolyte compositions

Low Salinity, Ionic strength 0,02		**High Salinity, Ionic strength 0,6**	
Without $CaCl_2$	With $CaCl_2$	Without $CaCl_2$	With $CaCl_2$
35 064 ppm NaCl	32 859 ppm NaCl 1 838 ppm $CaCl_2$	1 169 ppm NaCl	1 095 ppm NaCl 61 ppm $CaCl_2$

Surfactant concentration:

In order to make isotherms of adsorption as a function of surfactant concentration, 5 different concentrations were chosen per salinity. As mentioned in Chapter 3.1 Method, the concentration range has to be below CMC in order to calculate the difference in surfactant concentration from IFT measurements. Since the CMC is strongly dependent on the amount of electrolyte in solution (see chapter 2.3), the surfactant concentration range is also strongly dependent on the salinity. The concentration range for high salinity and low salinity samples were therefore different from each other. Table 3.3.2 shows the five surfactant concentrations which were selected for each of the salinities.

Table 3.3.2 Overview of the surfactant concentration chosen for each salinity

	Surfactant concentration [M] of Low Salinity, I = 0,02	Surfactant concentration of High Salinity, I = 0,6
#1	10^{-3}	$5*10^{-5}$
#2	$5*10^{-4}$	10^{-5}
#3	10^{-4}	$5*10^{-6}$
#4	$5*10^{-5}$	10^{-6}
#5	10^{-5}	$5*10^{-7}$

Aging time:

The pre-study revealed a vast variety results when it came to the time needed for adsorption to reach equilibrium. Mazen Ahmen Muherei and Radzuan Junin reported that 24 hours was enough to reach equilibrium for anionic and nonionic surfactants onto shale and sandstone [15], Zargham Salari et. Al. reported the same for adsorption of cationic surfactants onto carbonate rocks [16]. Other experiments performed by W. Zhou et al. used thirty days as a standard for letting adsorption reach equilibrium [14]. Although they used a different method for measuring concentration after equilibrium, the principle of time needed for equilibrium was the same. With such a wide range of results it was decided that aging time would be determined empirically.

As mentioned in Chapter 3.2 Procedure, six different time intervals were selected for the first method in determining the time it would take for the samples to reach equilibrium. Intervals of 5 minutes, 30 minutes, 60 minutes, 4 hours, 8 hours and 24 hours of mixing surfactant solution with kaolinite were chosen in addition to the reference sample without added kaolinite.

The specific time aging time for the samples using the second method was rather hard to calculate since the point of separation was hard to determine. The IFT was however measured instantaneously after mixing (with kaolinite in suspension), and then again after 5.5, 12, 17, 28 and 75 hours.

pH:

The pH of a typical reservoir is normally slightly acidic. The pH would usually increase by 1-3 units when injecting low salinity water [8]. The pH was not adjusted for the project. But in order for the Zeta potential measurements to have more applicability it was measured. The change in pH after thirty six hours of blending was also measured.

Kaolinite/Surfactant solution mixing ratio:

The samples were prepared in batches of 30 ml surfactant solution. 300 mg kaolinite was added to each batch. The amount of surfactant per gram kaolinite is therefore dependent on the surfactant concentration. This is presented in Chapter 4, Results and discussion.

Temperature and pressure

Both temperature and pressure were kept under normal conditions during the experiments. Room temperature of 22-24 °C and atmospheric pressure can be assumed.

3.4 Materials

Clay: Kaolinite

Chemical formula: $Al_2O_7Si_2*2H_2O$

Mw: 258,16 g/mol

The kaolin group is the most common clay mineral found in the K-feldspar-bearing sandstones. There are three subgroups of clay found within the kaolin group, kaolinite, dickite and nacrite [34]. ‘

Clays in general mainly consist of tetrahedral (T) and octahedral (O) building blocks- or sheets. The tetrahedral sheets have a basis in silicon-oxygen, while the octahedral can have a basis in either aluminum-, magnesium- or iron-oxygen structures. Altered combinations of these sheets, compose three main categories of two- or three-layered minerals; kaolinite, montmorillonite and ilite.

Kaolinite distinguishes itself from the other two categories by having a 1:1 ratio between tetrahedral and octahedral groups. Both ilite and montmorillonite has a 2:1 ratio where one octahedral sheet shares oxygen atoms with two silica sheets [35]. The octahedral layers of kaolinite have their basis in aluminum-oxygen structures.

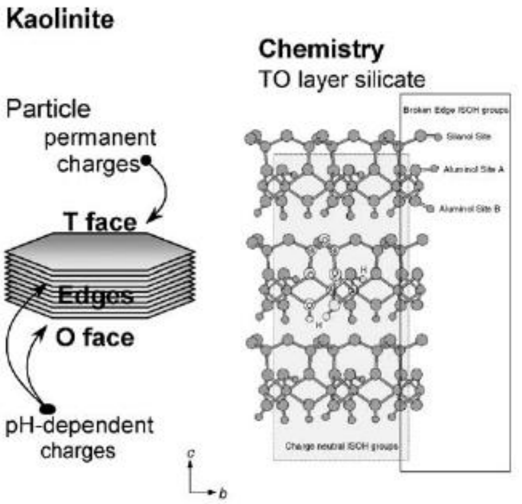

Figure 3.4.1 Illustration of kaolinite [35]

The fundamental planes of the kaolinite has a negative charge, however the layer charge density shows high variety and both negatively and positively charged parts on the surface exist simultaneously under acidic conditions. This is due to the conditionally charges sites located at the edges of the layers [35]. This is illustrated in Figure 3.4.1.

The kaolinite was delivered by Sigma-Aldrich.

Surfactant: Aerosol OT

Chemical Formula: $C_{20}H_{37}NaO_7S$

Mw: 444 g/mol

Aerosol OT is an anionic surfactant with two tails. It’s known for being an excellent wetting agent. As described in the introduction, it’s a Gemini surfactant, with two tails. This means that its likely to form other geometrical shapes than spheres when micellization occurs.

The Aerosol OT was delivered by Alfa Aestar and had a 96% purity.

3.5 Aparatus descrition

3.5.1 Zetasizer

Basic principle

As mentioned in Chapter 2.9 Zeta Potential, the electrical charge or charges of a particle interacts with an electric field. There are four distinct effects, also referred to as electrokinetic effects:

Electrophoresis: The movement of a dispersed particle under the influence of an electric field.

Electroosmosis: The movement of a liquid relative to a stationary charged surface, induced by an electric field.

Streaming potential: The electric field generated as a liquid flows past a stationary charged surface.

Sedimentation potential: The electric field generated as charged particles sediment.

The basic principle applied by the Malvern Zetasizer is measurements of the velocity of particles in a suspension, the electrophoretic mobility. If a system containing charged particles suspended in an electrolyte solution is subjected to an electric field, the particles would be attracted to the electrode of the opposite charge. The particles move towards the electrode of the opposite charge, viscous forces acts in the opposite direction and the velocity of the particle is constant when these two forces reach equilibrium. The velocity is dependent on the strength of the electric field, the dielectric constant of the medium, the viscosity of the medium, and the zeta potential of the particles. The Henry equation describes their relationship [32].

$$\mathrm{U_E} = \frac{2\varepsilon \mathrm{z} \mathrm{f}(\kappa \mathrm{a})}{3\eta}$$

Where U_E is the electrophoretic mobility, z = zetapotential, ε is the dielectric constant, η is the viscosity of the medium, and f(κa) is Henry's function. The Debye length κ is often taken as a measure of the "thickness" of the electrical double layer. "*a*" refers to the radius of the particle. (κa) therefore measures the radius of the double layer.

For systems with a moderate electrolyte concentration f(κa) is 1,5 and is referred to as the Scmoluchowski approximation. For systems containing small particles in a low dielectric constant media f(κa) becomes 1. This is referred to as the Huckel approximation.

The Zetasizer Nano Series uses a combination of laser Doppler velocimetry and phase analysis light scattering to measure the particle electrophoretic mobility.

Apparatus description:

The zeta potential measuring system has a laser which is used to illuminate the particles within the sample. This light source is split to provide an incident and reference beam. The incident beam passes through the sample and scattered light of about 13° is detected. The cell is subjected to an electric field, causing electrophoresis. Any particles moving through the measurement volume will cause the intensity of the light detected to fluctuate in a frequency proportional to the particle speed. The Zetasizer Nano software will calculate the zeta potential based on the measured electrophoretic mobility. The Zetasizer Nano uses an attenuator to secure that the intensity of the detected scattered light is within the limits of the detector.

Concentration Limits

The concentration limits of the Zetasizer Nano is not easy to define. This is due to the multiple parameters which defines these limits. Ultimately the limit will have to be determined empirically by measuring the samples at different concentrations and analyzing the effect on the data quality obtained. In general the limits are affected in the following ways [36]:

- Larger particle size, lower the minimum and maximum particle concentration at which the sample can be successfully measured.
- Vice versa smaller particles allow for a higher particle concentration.
- A lower relative refractive index allows for a higher particle concentration.

The apparatus’s limitations regarding electrolyte composition is also a parameter which had to be determined empirically. As later described in the Chapter 4, Results and Discussion, the high salinity samples were considered to have too high electrolyte concentration.

3.5.2 Sigma 70 Tensiometer

A sigma 70 tensiometer delivered by KSV instruments was used for measuring the interfacial tension. This apparatus measures the interfacial tension between two fluids by measuring the force inhibited on a probe which interacts with both fluids. The probe is hung on a balance and the force measured by the balance is used to calculate the interfacial tension. The mathematical interpretation of the measured force depends on the shape of the probe.

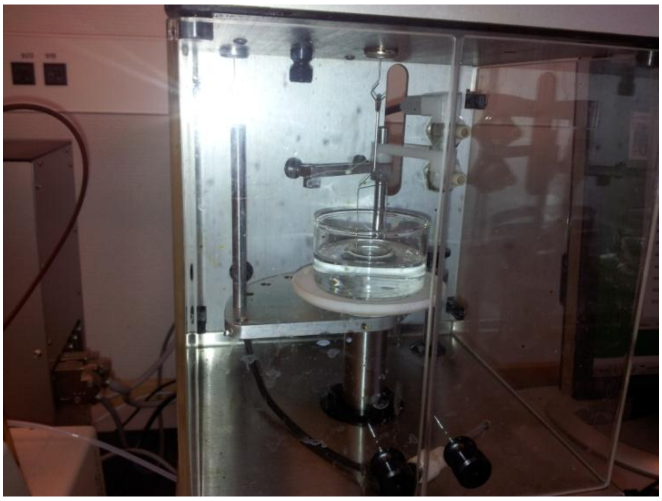

Figure 3.5.1 Picture of the Sigma 70 Tensiometer during measurement of a sample.

A Du Noüy Ring has been used for the experiments carried out during this project. This method utilizes a platinum ring which is submerged below the interface and into the heavy phase. The ring is then slowly pulled upwards towards the interface and into the light phase. A meniscus is formed as the ring is pulled further into the light phase. As the meniscus is pulled further into the light phase, it will exert a force onto the balance which the ring is attached to. Eventually the meniscus will break and return to its original form, but prior to this event, a maximum is achieved and the force measured by the balance decreases. When the tensiometer detects the maximum, the ring is returned to the heavy phase. A schematic overview with a following description of the different steps of the process is shown below [37]:

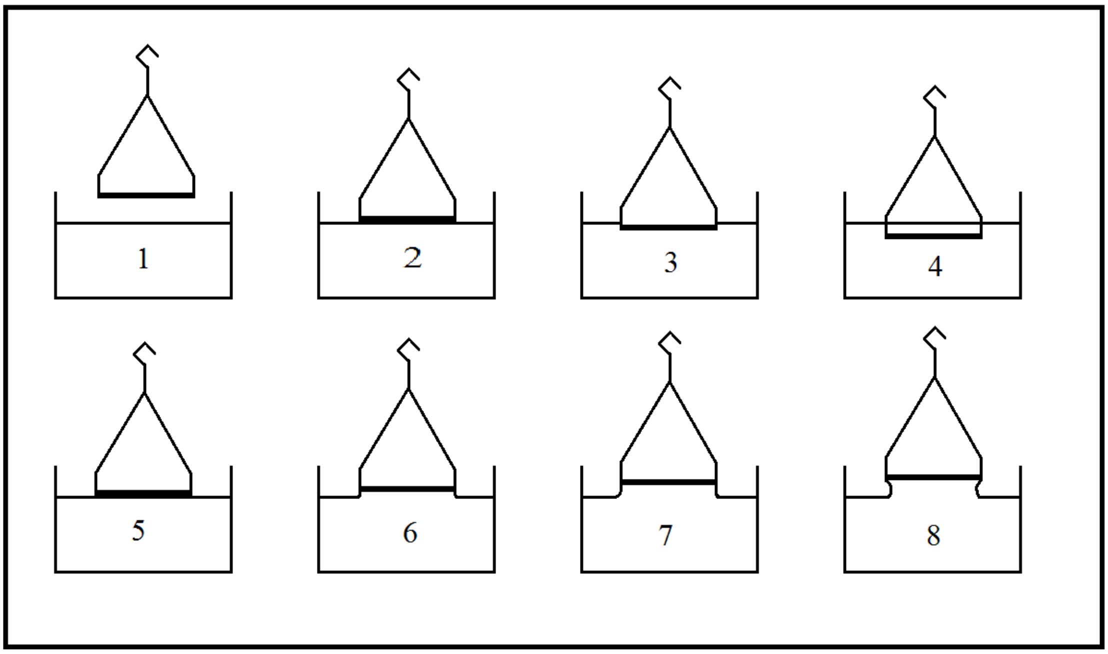

Figure 3.5.2 Schematic overview of the measuring steps of the tensiometer.

1) The ring is above the surface and the balance is tared.
2) The ring connects with the interface and there is a small increase in force caused by the adhesive force between the ring and the interface.
3) A small negative force is needed as the ring is pushed through the interface
4) After the ring has been pushed through the interface a small positive force is measured due to the supporting wires of the ring.
5) The ring re-enters the interface and the force starts to increase.
6) The force keeps increasing as the meniscus is pulled upwards
7) The peak force is reached
8) A small decrease in force is measured before the meniscus breaks.

Before any experiments are conducted with the Sigma 70 tensiometer, the calibration of the apparatus is tested with water. The requirements is that it’s calibrated within +/- 1 [mN/m] for pure water.

The calculations:

The force that is inhibited on the platinum ring if it's completely wetted is given by the following equation [20]:

$$F_t = W_r - b + 2(2\pi r\gamma)$$

Where F_t is the measured force inhibited on the ring, W_r is the weight of the ring in the light phase (which for these measurements would be air), b is the buoyancy, r is the radius of the ring and γ is the interfacial tension. The factor of 2 in the last part of the equation is included as the liquid is in contact with the rings both inner and outer perimeter.

Position four in the illustrations shown in Figure 3.5.2 would be the starting position of measurements when using the tensiometer. The weight of the ring (W_t) and the buoyancy (b) will then be zeroed or tarred out before starting the measurements. The net force inhibited onto the ring is then given by:

$$F = 4\pi r\gamma$$

This equation is however likely to deviate from the actual force inhibited due to the complex nature of the meniscus. These calculations do not consider the additional volume of liquid which is raised due to proximity of one side of the ring to the other. The mathematical correction is made by adding a correction factor. Three different correction factors has been suggested for this purpose; Harkins and Jordan's, Zuidema and Waters's, and Huh and Mason's. The latter one is the one which has been used for the Sigma 70 tensiometer. The interfacial tension is at last given by:

$$\gamma = \frac{K * F}{4\pi r}$$

Where K is Huh and Mason's correction factor.

3.6 HSE

A risk assessment was carried out before using any of the apparatus. This is a form which maps and evaluates the activities that were considered to be risky. The risk assessment was carried out in cooperation with the supervisor. The risk assessment for this project is attached in Appendix A.

4 Results & Discussion

This chapter sums up the results that were found during the course of the project. A registered change in IFT over time during the measurements will be discussed before the CMC plots and equations for how the IFT varied with the surfactant concentration will be presented. Followed by this, the results of the adsorption studies will be shown. An interpretation of the results is also given in this section. In the last section the zeta potential results in addition to a summary to sum it all up.

4.1 Change in IFT over time

One of the central problems was that the IFT changed over time while measuring samples with the Du Noüy Ring tensiometer. If this was a cause of diffusion of surfactants or contaminations to the interface is uncertain. Another cause could be adsorption of components onto the Du Noüy Ring. The measurements seemed to be most sensitive at very low surfactant concentrations. Figure 4.1.1 illustrates the progression of the IFT measurements at very low surfactant concentrations.

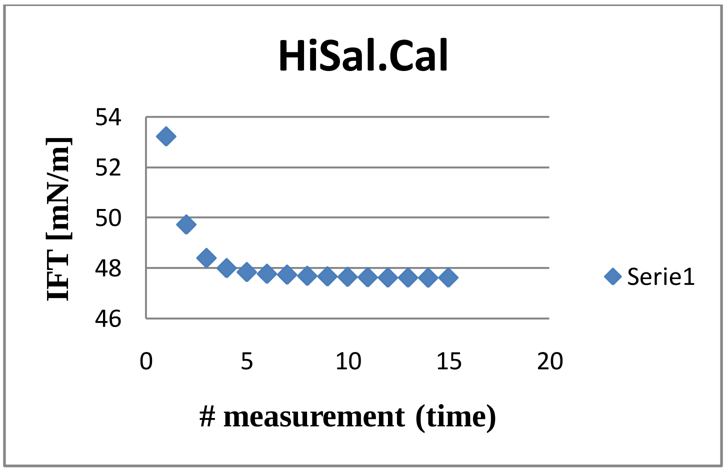

Figure 4.1.1 Illustration of how IFT chaanges with time during measurements. #7x sereies, of hight salinity samples with calsium after 5 minutes.

By the progression of IFT illustrated in Figure 4.1.1, it’s easy to assume that diffusion of components which reduce the IFT diffuse to the interface. However, another progression of IFT as a function of time was also registered. This is illustrated in Figure 4.1.2.

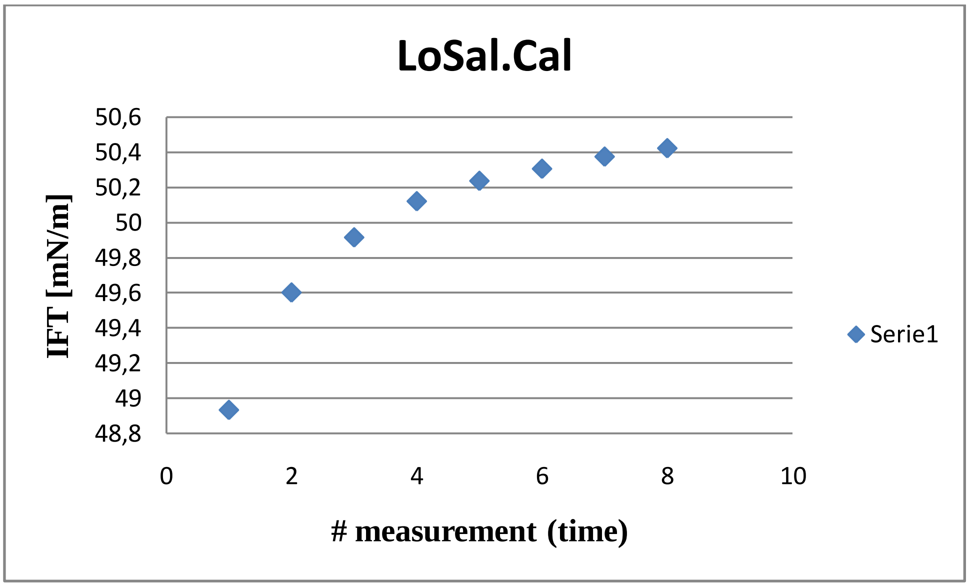

Figure 4.1.2 illustration of how IFT changes with time during measurements, #6x series, low salinity with calcium sample.

The data which has been presented in this report (also shown in Appendix B-G) are the IFT logged after the equilibrium with respect to time has been reached. Whether this data is the best to represent the bulk solution is uncertain. According to the theories presented in Chapter 2.1.2, Diffusion, IFT changes over time, the best representative might be the first logged data point. However, in order to be consistent with the data which has been presented, the equilibrium IFT is the data that has been presented.

4.2 Determination of CMC

As mentioned in Chapter 3, Materials and Methods, the surface tension method of measuring adsorption is reliant upon knowing both the CMC, and how IFT changes as a function of surfactant concentration. Defining the CMC for the different salinities was therefore the first priority.

The CMC was found by measuring the IFT for varied concentrations of Aerosol OT in each of the four salinity solutions. Since the CMC was unknown beforehand, and no literature obtained was able to point towards a likely CMC, this was done in a try-and-fail manner. Nine different surfactant concentrations were selected and measured for each of the four salinities.

Low Salinity:

The interfacial tension was measured for nine samples of different concentrations. The results were plotted and revealed a breaking point in interfacial tension between 0,0005 and 0,0015 Mol AOT concentration. The plot for IFT of AOT under low salinity conditions are shown in Figure 4.2.1:

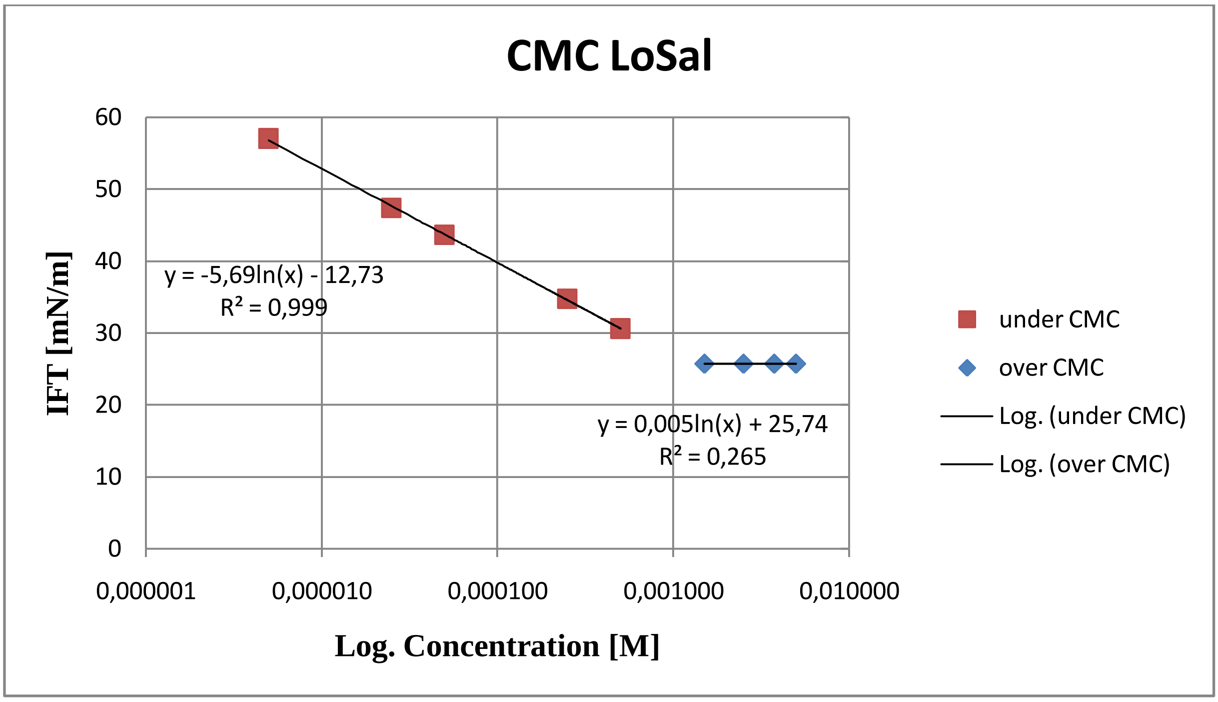

Figure 4.2.1 CMC plot for Aerosol OT in low salinity conditions.

Microsoft Excel was used for estimating an equation for the trend lines over and under CMC. The CMC was calculated as the point where the equations were equal to each other and solved for x. CMC for Aerosol OT under low salinity conditions was calculated to be $1{,}165 \cdot 10^{-3}$ Mol. It was just as important to know the equation for IFT as a function of surfactant concentration under CMC as was used for calculating surfactant concentration under the adsorption studies.

Low salinity with calcium

The CMC plot for Low salinity conditions with calcium was created in the same way as for the CMC plot for low salinity conditions. The plot for IFT of AOT under low salinity conditions with calcium are shown in Figure 4.2.2:

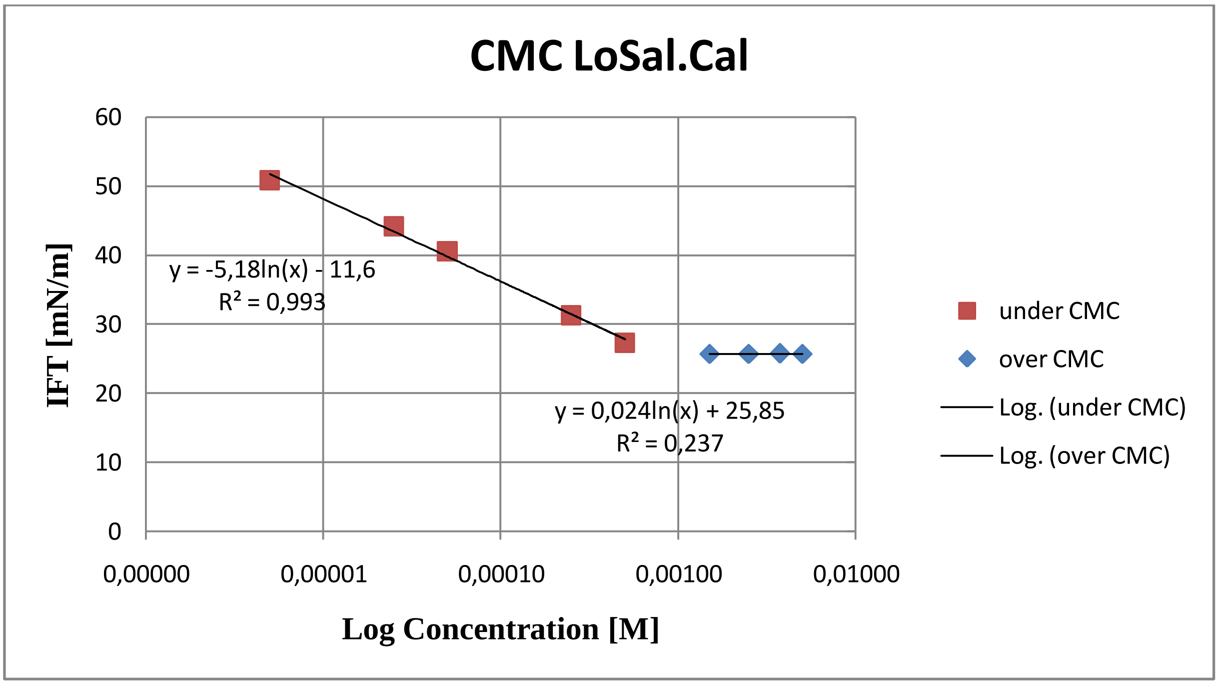

Figure 4.2.2 CMC plot for Aerosol OT under low salinity with calcium.

The CMC was calculated to be 7,49*10^{-4} Mol Aerosol OT. Although the ionic strength of these solutions was the same, the divalent calcium reduced the CMC of surfactant in the solution.

HiSal:

In the same manner as for both of the low salinity solutions, the CMC plot for high salinity solutions were plotted by measuring IFT at different surfactant concentrations. According to the theory presented in Chapter 2.3 Critical Micelle Concentration, increasing the electrolyte concentration should greatly reduce the CMC. The plot for IFT of Aerosol OT under high salinity conditions are shown in Figure 4.2.3:

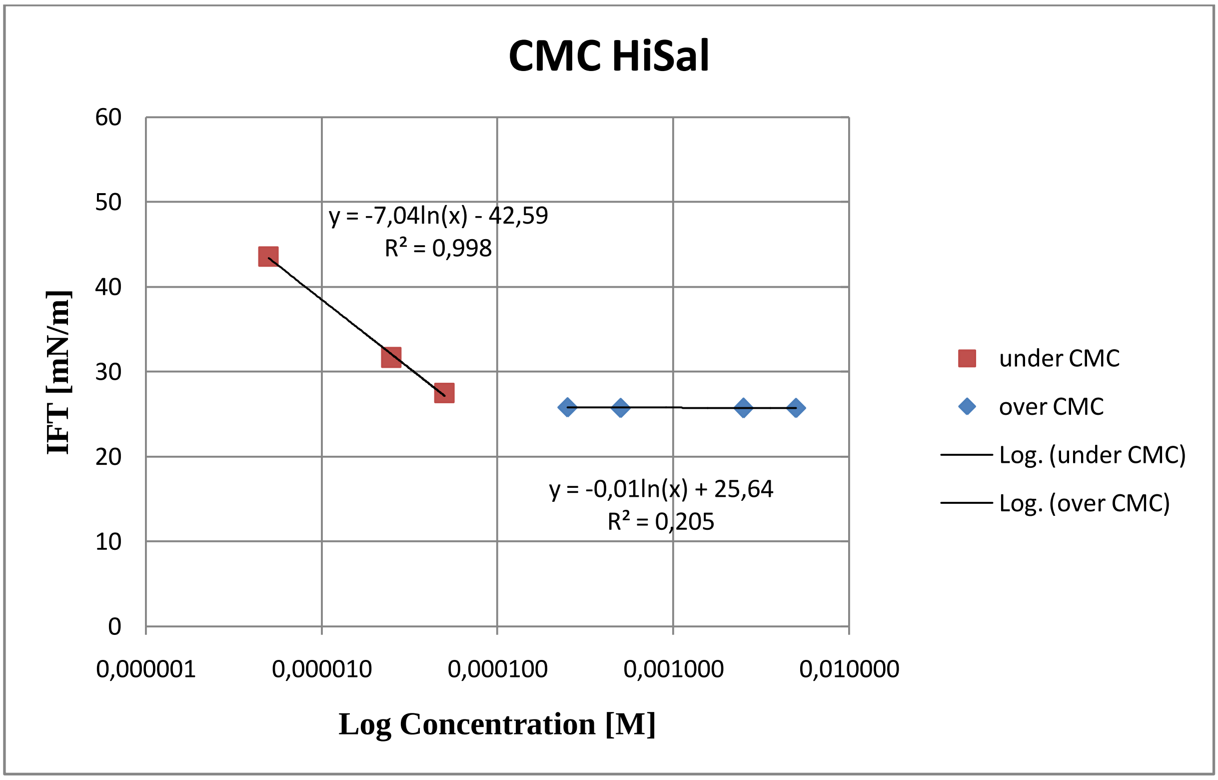

Figure 4.2.3 CMC plot for Aerosol OT under high salinity conditions.

As expected the IFT shows a breaking point at a much lower concentration than for both of the low salinity conditions. The calculated CMC for AOT under high salinity conditions was $6{,}09*10^{-5}$ Mol.

HiSal.Cal:

Judging from the results of the previous experiments, the CMC was expected to be lower than for the other salinities. The results are shown in Figure 4.2.4.

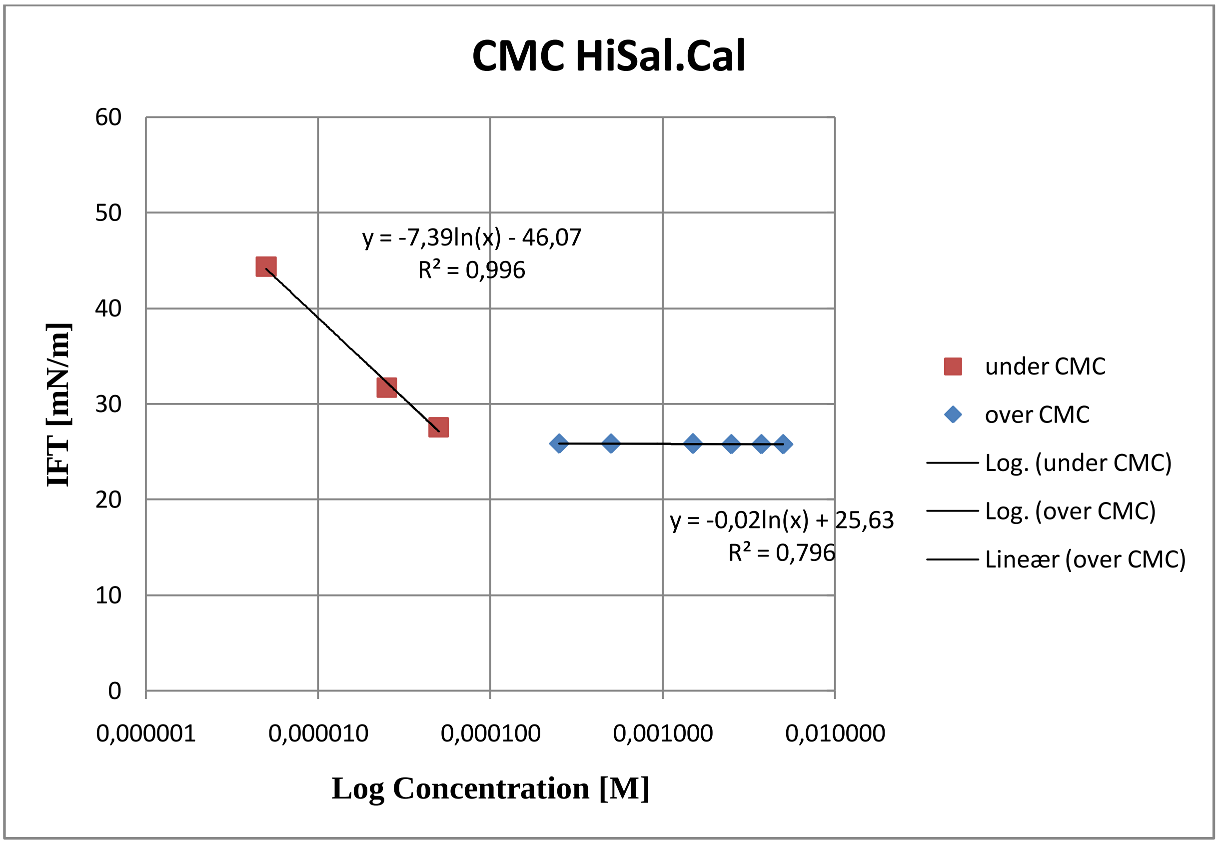

Figure 4.2.4 CMC plot for High salinity with Calcsium.

The CMC for Aerosol OT under high salinity conditions was calculated to be 5,96*10^{-5} M. The same trend that was observed for the CMC plots of lower ionic strength solutions was also observed for the solutions of higher ionic strength. The divalent calcium ions further reduce the CMC even at equal ionic strengths.

Summary:

The CMC was measured under four different salinity conditions. Higher ionic strength reduced the CMC of aerosol OT. The same effect was observed for addition of calcium. The presence of divalent cations further reduced the CMC, even if the ionic strength of the solution was the same. The equations that describe the change in IFT as a function of surfactant concentrations will be used for calculating the amount of adsorbed under the adsorption studies. An overview of these equations and the related CMCs are given in Table 4.2.1:

Table 4.2.1Overview of CMC and equations describing change in IFT(y) as a function of Concentration(x)

Salinity	CMC [Mol]	Equation, IFT(y) = f(Concentration(x))
Low salinity	$1,165*10^{-3}$	$y= -5,69\ln(x)-12,63$
Low salinity with calcium	$7,49*10^{-4}$	$y= -5,18\ln(x)-11,6$
High salinity	$6,09*10^{-5}$	$y= -7,04\ln(x)-42,59$
High salinity with calcium	$5,96*10^{-5}$	$y= -7,39\ln(x)-46,07$

4.3 IFT measurements

As mentioned in Chapter 3.2 Procedure, there were two different procedures of executing the adsorption studies. The first procedure was assessed to give the most reliant results and will thus be the one presented as the actual adsorption results. A comparison between the two methods and a justification of why the first method was preferred over the second will be given.

4.3.1 Comparison first and second method

As mentioned in Chapter 3.2 Procedure, two different methods were used for studying the adsorption. Both of these methods showed the same trend of adsorption. The two highest concentrations of surfactant for the High salinity series was selected for illustrating the similarities between the methods.

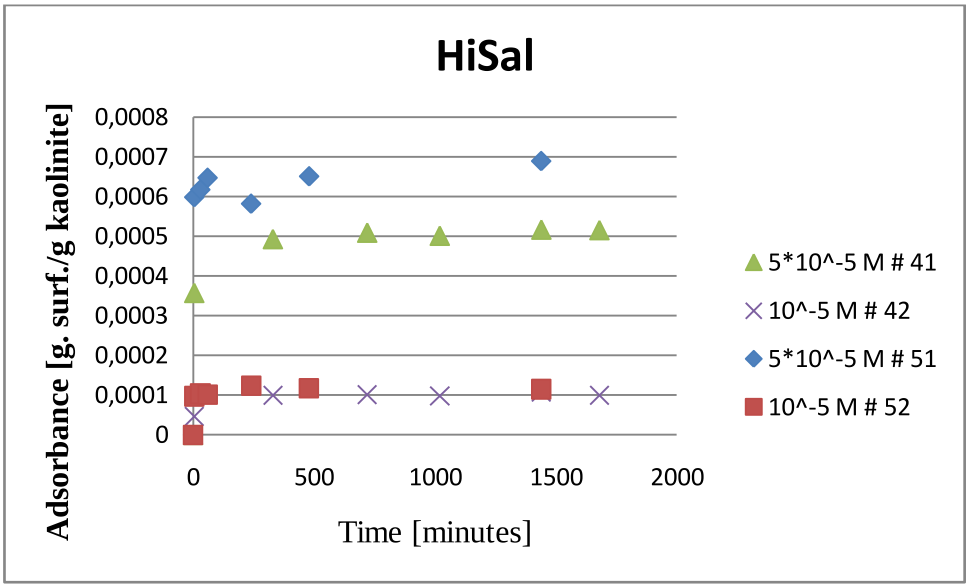

Figure 4.3.1 Adsorption of experiments performed with the first method (#51, #52) and the second method (#41, #42).

The #51 and #52 series were conducted using the first method, which were separated with the centrifuge, whilst #41 and #42 series were conducted using the second method. As illustrated by Figure 4.3.1, the second method where the samples weren't centrifuged for separation shows slightly lower adsorption. When using this method, kaolinite was still present in the solution when measuring the IFT. This is shown by Figure 4.3.2.

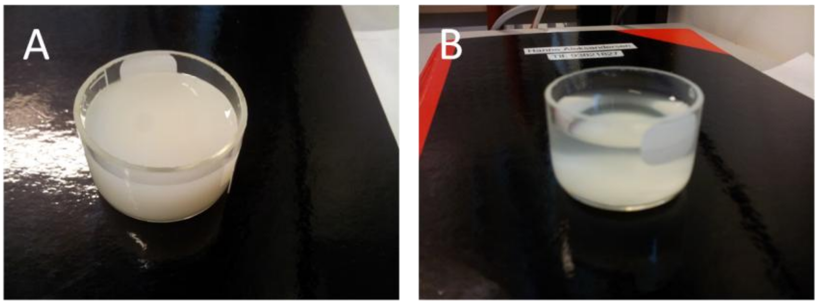

Figure 4.3.2 Picture of the beakers used for measuring IFT. A) illustration of sample with kaolinite suspended in the solution. B) Sample after the sample was left to sediment for 5 hours, kaolinite is still present in solution.

In comparison the samples which were conducted using the first method, with centrifugation were separated to a much higher degree. These samples did however suffer a higher risk of contamination due to the multiple switching of vessels. Figure 4.3.3 shows the samples before and after the samples were centrifuged.

Figure 4.3.3 Picture of samples before and after centrifuge. the kaolinite packs tightly at the bottom as illustrated.

In the end the series which were centrifuged were considered to give the most reliable results. Due to the limitations experimental procedure when it comes to measuring IFT at very short timescales, the adsorption equilibrium time wasn’t studied, and thus the exact time of separation wasn’t as crucial as first assumed. The degree of separation was however the deciding factor for why the first method was preferred.

4.3.2 Adsorption results

Five concentrations per salinity were selected for adsorption studies. As earlier mentioned, these concentrations were selected and limited by the CMC of AOT for each of the salinities. For each of these concentrations six durations of adsorption were selected in addition to a reference sample without added kaolinite. This was done to get a measurement of how fast adsorption would reach equilibrium.

Low salinity:

The results for the low salinity samples revealed quite confusing results. First, the equilibrium time seems to be close to or less than five minutes which is the shortest interval of mixing kaolinite and surfactant solution before separation. For the higher surfactant concentrations the IFT actually increases after the solution has been mixed and separated from the kaolinite.

By the calculations shown in Chapter 4.2, this would indicate that something desorbs from the kaolinite and thus reduces the IFT. A possibility is that traces of kaolinite were still suspended in the solution even after separation and that this decreases the IFT. (This should however affect all the samples.) The results are presented in figure 4.3.4

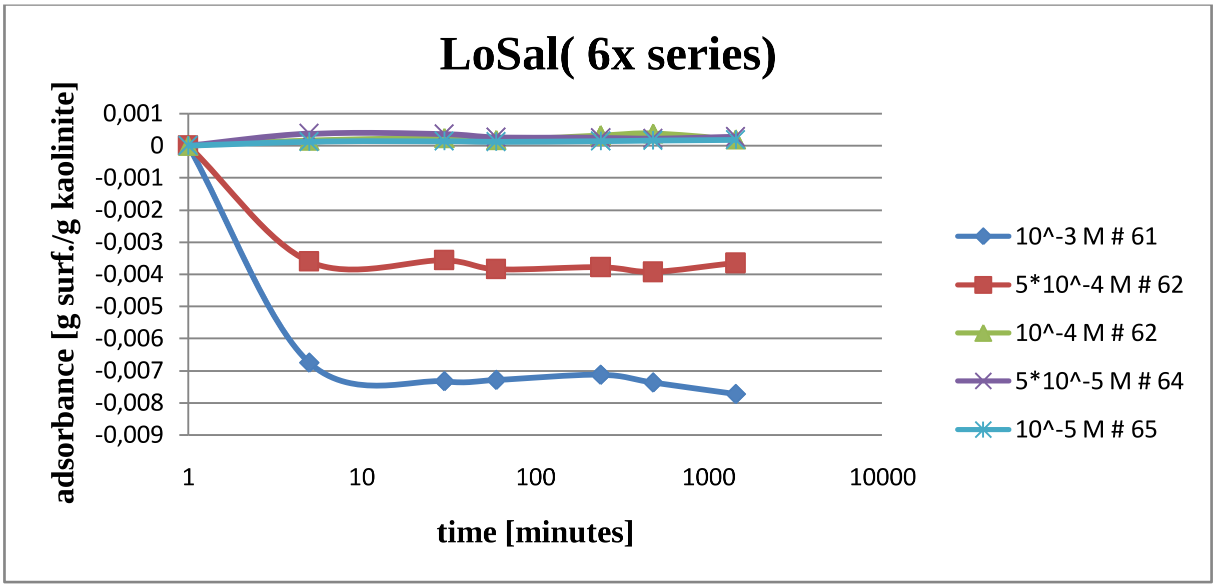

Figure 4.3.4 adsorption results, Low salinity without calcium

The low salinity series was retested due to the suspicious results. The results of the parallels are shown in Figure 4.3.5. Although the measurements show more noise for the higher surfactant concentrations of the second measurements, the general behavior was the same as for the first low salinity samples. A probable cause of error could be that the highest surfactant concentrations of the low salinity samples were too close to the CMC and that the fitting of the equation is poorer in this concentration range.

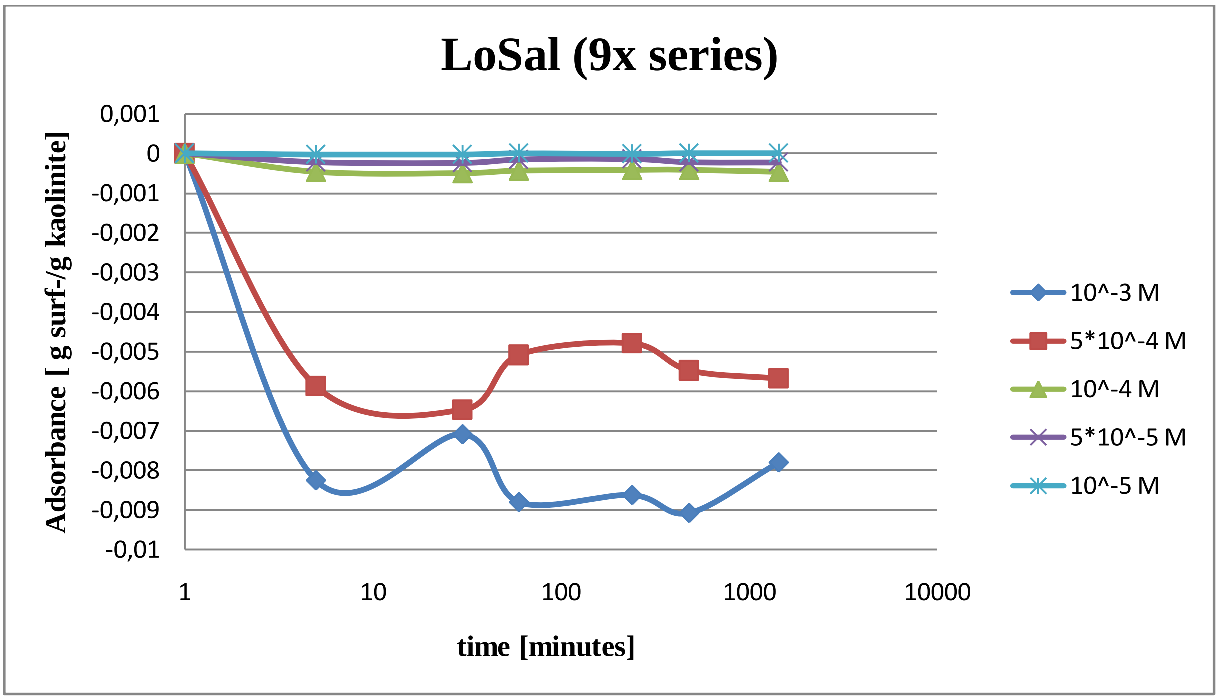

Figure 4.3.5 adsorption results, parallel of Low salinity without calcium

Low salinity with calcium:

The low salinity samples with calcium were prepared and measured in the exact same way as the low salinity samples. The similarity of the CMC for the two solutions allowed for the concentration range of surfactant to be the same as well. The results are shown in Figure 4.3.6

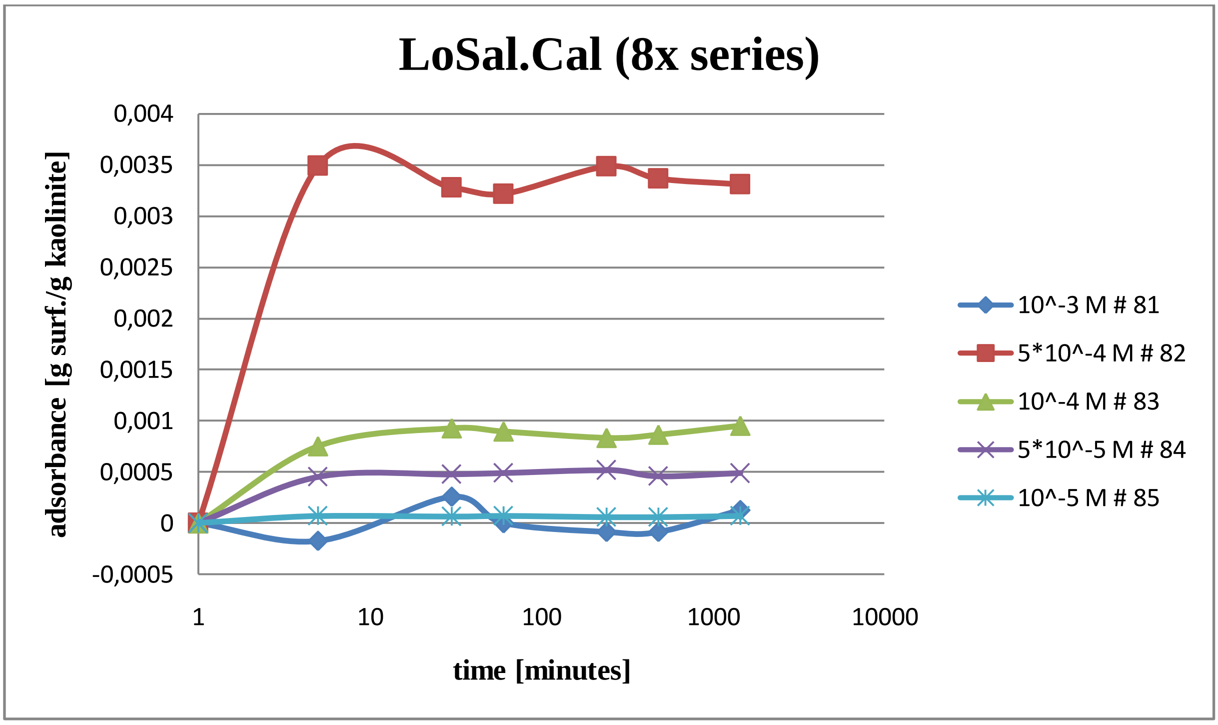

Figure 4.3.6 adsorption results, Low salinity with calcium

The result for the highest concentration, sample #81, clearly deviates from the general trend of the other measurements. By overlooking this sample, the general trend is that higher surfactant concentration yields higher adsorption. Sample #81 was retested in the same manner as the low salinity samples were retested and the result was the same. The time it takes to reach equilibrium seems to be the same as for the low salinity series without calcium, close to five minutes or less.

High salinity:

The execution of testing the high salinity samples was the same as for both of the low salinity series. The change here is a lower surfactant concentration due to a lower CMC. The concentration range for the high salinity series was from $5*10^{-7}$ to $5*10^{-5}$ M AOT. The results are shown in Figure 4.3.7.

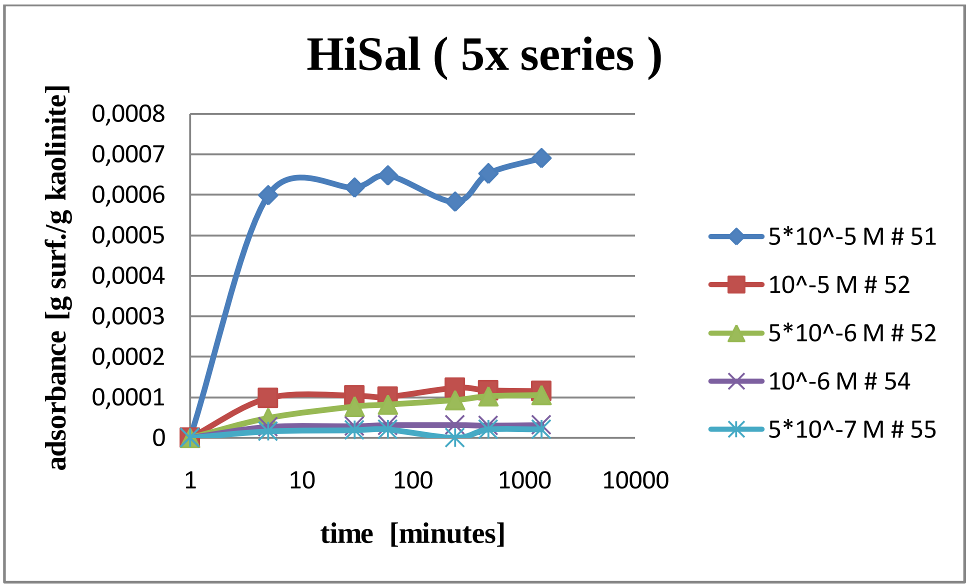

Figure 4.3.7adsorption results, High salinity without calcium

The same general trend of higher surfactant concentration yielding higher surfactant adsorption per gram kaolinite that was observed for the low salinity series with calcium is also observed for the high salinity series. Increasing the surfactant concentrations seems to also increase the amount adsorbed onto kaolinite.

High salinity with calcium:

The series of high salinity with calcium was carried out in line with all the other series. The general trend here was the same as for the high salinity and low salinity with calcium series. Increased surfactant concentration seemed to yield higher adsorption. The results are shown in Figure 4.3.8:

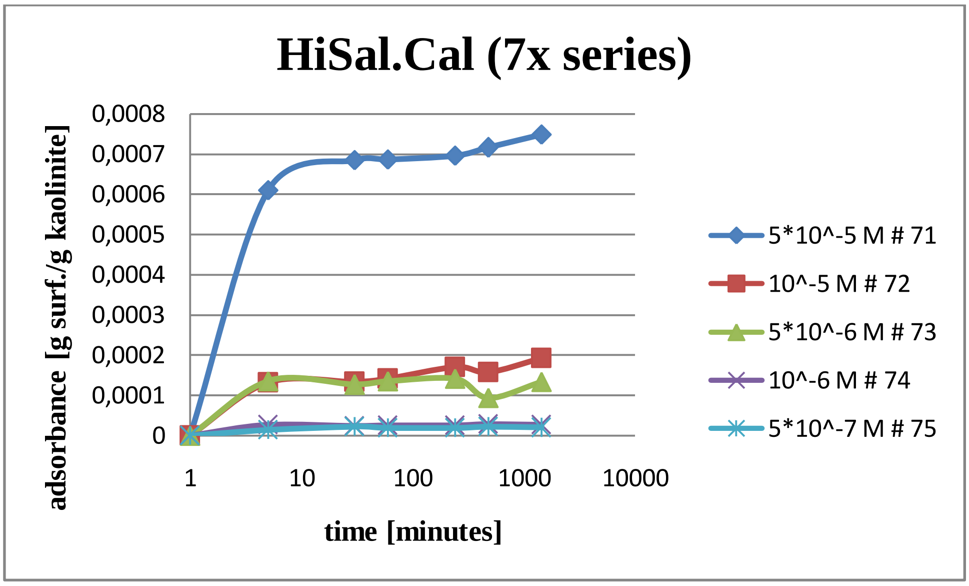

Figure 4.3.8 adsorption results, High salinity with calcium

The amount of adsorbed surfactant for the high salinity series with calcium seems to be very similar to the amount adsorbed for the high salinity series without calcium. This was expected as the Ionic strength was the same for both solutions. If any trend of deviance from the high salinity series is to be noted, it would be a slightly higher amount adsorbed for the series with calcium.

4.3.3 Comparison HiSal Low Sal

In comparison with the low salinity series with calcium there are only two measured sample with the same concentration. These are the 5*10^{-5} Mol and the 10^{-5} Mol samples. This is shown in figure 4.3.9

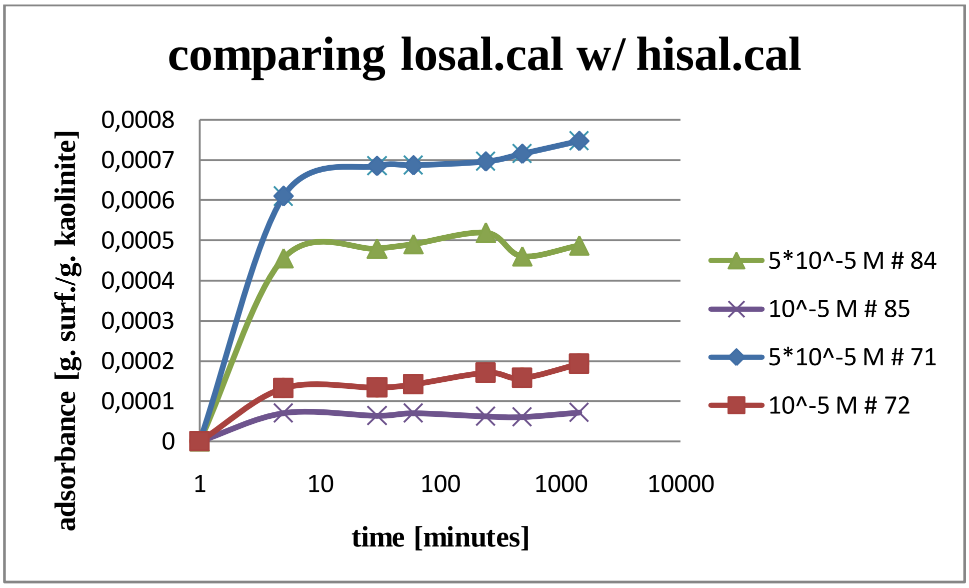

Figure 4.3.9 Comparison of adsorption between low salinity with calcicum (#84 and #85), and high salinity with calcium (#71 and #72).

The green trend (#84) is the calculated adsorption of the series with low salinity and calcium. When comparing this to the high salinity series with calcium (#71) of the same concentration, it's clear that the calculated adsorption is increased for the solution of higher ionic strength. This is in line with the general theory of how surfactant adsorption is dependent on the electrolyte concentration. The same trend is observed for the lower surfactant concentration samples of both salinity series. The sample with higher ionic strength, #72, shows a higher calculated adsorption than the sample of lower ionic strength but same surfactant concentration, #85.

Comparison between the high and low salinity series without calcium yield similar result for the samples of highest concentration, $5*10^{-5}$. However, the trend was somewhat different for the samples with lower surfactant concentration. This is shown in Figure 4.3.10:

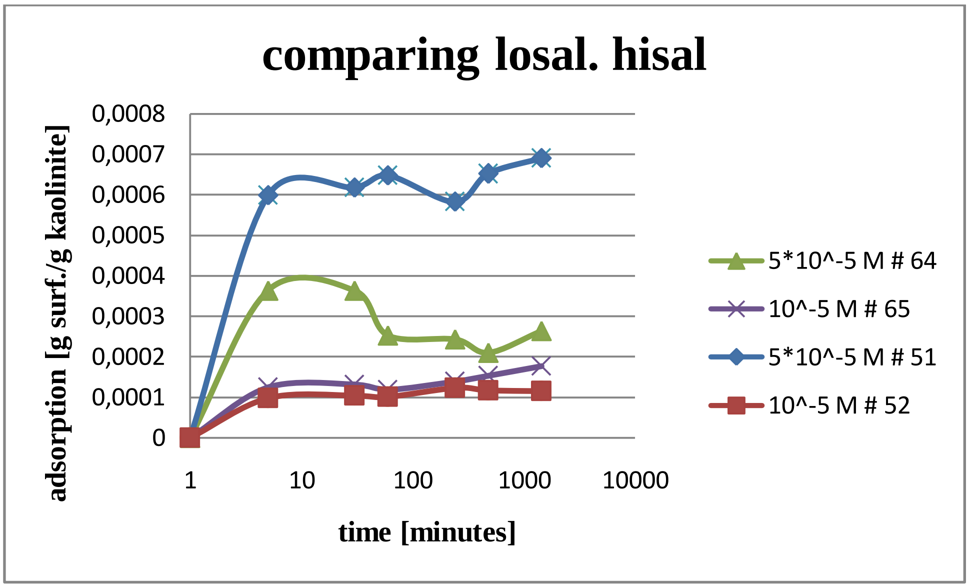

Figure 4.3.10 comparison of adsorption between low salinity without calcisum (#64 and #65) and high salinity without calcium (#51 and #52).

The general trend spotted so far has been that increasing the salinity/electrolyte concentration promotes adsorption of AOT onto kaolinite. This was not the result when the high and low salinity samples of $10^{\wedge-5}$ Mol AOT were compared. As shown in figure X, the high salinity sample, #52, had slightly less adsorption than the low salinity sample, #65. The difference is however very small.

4.3.4 Adsorption isotherm

In this chapter, the results that were presented in chapter 4.3.2, Adsorption results, are plotted as isotherms. This was done by calculating the average value of adsorption from the adsorption vs. time plots, and plotting them as a function of surfactant concentration. This way the adsorption results are presented as isotherms in the same manner as mentioned in chapter 2.8.2, adsorption isotherms. The adsorption isotherms for the high salinity series, with and without calcium are presented in Figure 4.3.11.

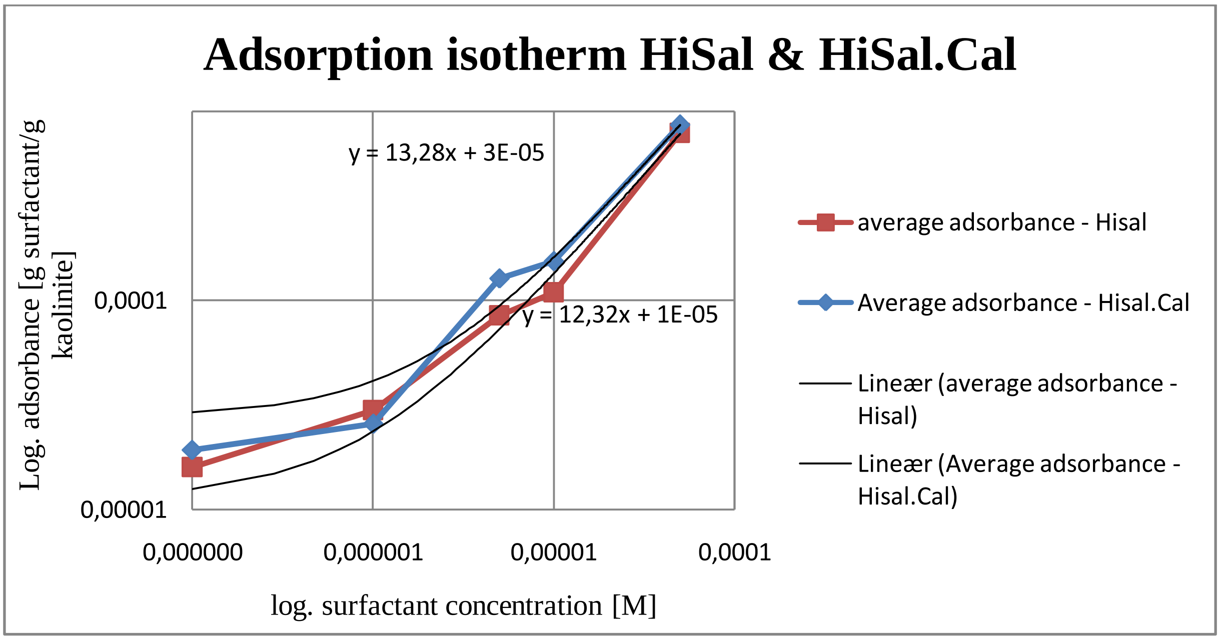

Figure 4.3.11Adsorption isotherms of High salinity samples with and without calcium

The isotherms were plotted in the log/log scale, and the linear equations, describing the average overall slope of the plots are attached. The same was done for the low salinity series with and without calcium. This is shown in Figure 4.3.12.

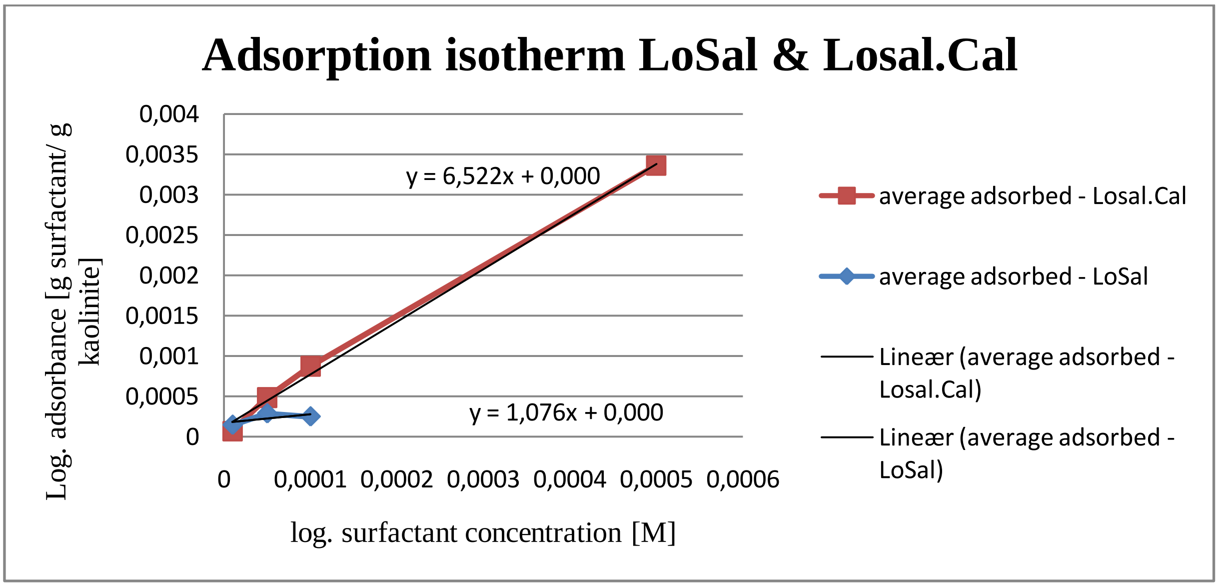

Figure 4.3.12 Adsorption isotherms of Low salinity samples with and without calcium.

The isotherms illustrating adsorption as a function of surfactant concentration are a bit more amputated for the low salinity series, both with and without kaolinite. This was done due to the off results presented in chapter 4.3.2 Adsorption results. This of course reduces the quality of the data presented in the isotherm.

Summary:

The adsorption isotherms do not show any clear breaking points in adsorption as a function of surfactant concentration. The trend is however as pointed out in chapter 4.3.4, that the lower salinity series has a lower slope number than for the high salinity series which again means smaller increase in adsorption as a function of surfactant concentration. Without a clear break in slope it’s difficult to propose a mechanism of adsorption over the concentration range.

4.4 pH measurements

The pH was measured to see if there was any significant change after adding kaolinite to the solutions. The pH was therefore measured in pure surfactant solution with various salinities and surfactant concentrations, and re-measured thirty six hours after adding kaolinite. The results are presented in Appendix I. The results did not display any large changes in pH after thirty six hours.

4.5 Zetapotential

The zetapotential was measured for both high salinity series with and without calcium, and the low salinity series with and without calcium. The zetapotential measurements are however sensitive to the amounts of electrolyte in the suspension. The results of the high salinity series with and without calcium had very much noise and were therefore disregarded. The results of the low salinity series with and without calcium are shown in Figure 4.5.1:

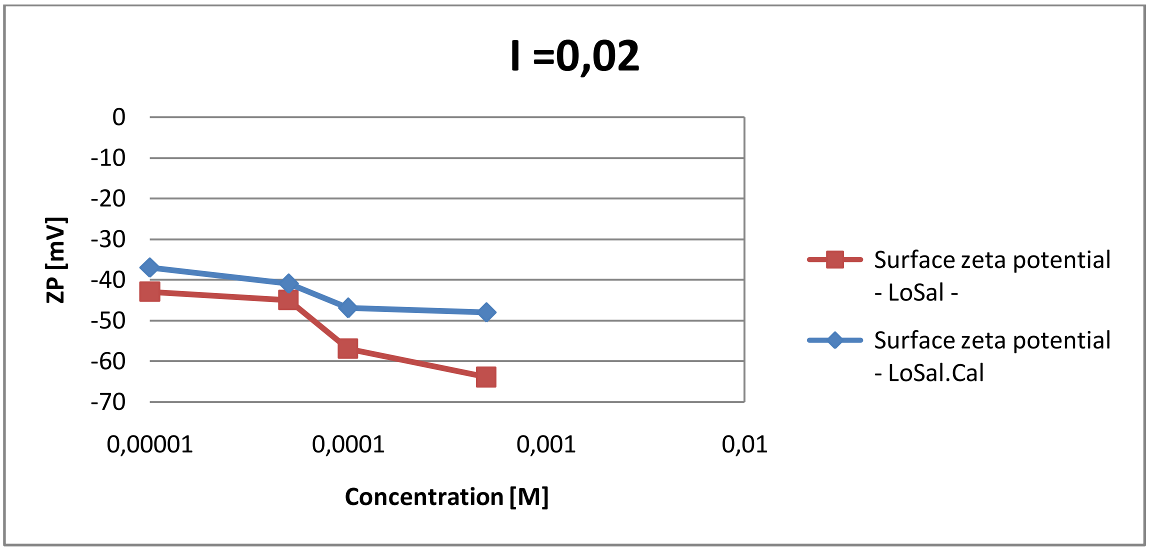

Figure 4.5.1Surface zeta potential as a function of surfactant concentration for low salinity samples, with and without calcium.

The magnitude of negative surface zeta potential was generally higher for the low salinity series without calcium than for the series with calcium. For both trends the surface zeta potential becomes more negative as the surfactant concentration increases. If the anionic AOT adsorbs at the surface of the kaolinite particle, this would likely lower the surface zetapotential. The enlarged negative magnitude of surface zeta potential as a function of surfactant concentration is thus an indication that AOT does adsorb at the surface of kaolinite.

The fact that the samples without calcium had a larger negative magnitude of surface zeta potential than the samples with calcium should indicate a higher amount of adsorption for the series without calcium. This is not reflected by the surface tension measurements presented in chapter 4.2.

5 Conclusions

Adsorption of the anionic surfactant, Aerosol OT, onto kaolinite has been studied. The indirect method of measuring surface tension to determine the surfactant concentration has been applied for this purpose. In general most of the results that were found suggested that Aerosol OT does adsorb onto kaolinite. The exception was the experiments performed under high surfactant concentrations and low salinity solutions. The results of having a higher salinity/electrolyte concentration agrees with the theory presented, increased ionic strength promotes adsorption. The results of the surface zetapotential measurements that were conduced support the theory of anionic Aerosol OT adsorption onto kaolinite.

The indirect method of measuring surface tension to determine surfactant concentration allows for quick and easy measurements, but at the cost of some accuracy. The apparatus is calibrated to +/- 1 [mN/m] which allows for a noteworthy error at higher surfactant concentrations. Additionally, IFT-measurements over time suggest that diffusion to and from the interface occur during measurements.

Due to all the mentioned factors, the adsorption values which have been presented should not be considered to be exact. However, what should be extracted from the results are the tendencies which have been presented.

Even though the surface tension method has been applied by others who have been studying similar scenarios of surfactant adsorption, the accuracy and validity of this method remains questionable. There is room for many sources of error and to really conclude and verify the results performed during this project, more experiments should be conducted.

6 References

1. M. Sohrabi, D.H.T., A. Danesh, G.D. Henderson, Heriot-Watt U, *Visualization of Oil Recovery by Water-Alternating-Gas Injection Using High pressure Micromodels.* SPE Journal, 2004. **9**(3): p. 390-301.
2. Christensen Jes Reimer, S.E.H., Skauge Arne, *Proceedings of the SPE/DOE Improved Oil Recovery Symposium.* Society of Petroleum Engineers, 1998: p. 233-248.
3. J.J Taber, F.D.M., R.S. Seright, *EOR Screening Criteria Revisited - Part 1: Introduction to Screening Criteria and Enhanced Revovery Field Projects.* SPE Reservoir Engineering, 1997. **12**(3): p. 189-198.
4. Butler, R.M., *Thermal Recovery of Oil and Bitumen.* 1991: p. 1-27.
5. Jean-Louis Bantignies, C.C.D.M., and Hervè Dexpert, *Wettability contrasts in kaolinite and illite clays: Characterization by infrared and X-ray absorption spectroscopies.* Clays and Clay Minerals, 1997. **45**(2): p. 184-193.
6. Sanchez, N.L., *Management of Water Alternating GAS (WAG) Injection Projects.* Society of Petroleum Engineers, Conference Paper, 1999.
7. Y. Zhang, X.X., N. R. Morrow, *Waterflood Performance by Injection of Brinw With Different Salinity for Reservoir Cores.* Society of Petroleum Engineers, Conference Paper, 2007.
8. Tor Austad, A.R.a.T.P., *Chemical Mechanism of Low Salinity Water Flooding in Sandstone Reservoirs.* Society of Petroleum Engineers, Conference Paper, 2010.
9. Ramirez A. Nasralla, H.A.N.-E.-D., *Double-Layer Expansion: Is It A Primary Mechanism of Improved Oil Recovery by Low-Salinity Waterflooding?* Society of Petroleum Engineers, Conference Paper, 2012.
10. Don W. Green, G.P.W., *Enhanced Oil Recovery.* Society of Petroleum Engineers, 1998: p. 240-243.
11. F. M. Menger, C.A.L., *Gemini Surfactants: A New Class of Self-Assembling Molecules.* J. Am. Chem. Soc., 1993. **115**(22): p. 10083-10090.
12. Bo Gao, M.M.S., *A New Family of Anionic Surfactants for EOR Applications.* Society of Petroleum Engineers, Conference Paper, 2012.
13. Adlercreutz, P., *Immobilization and application of lipases in organic media.* Chem Soc Rev, 2012.

14. W. Zhou, M.D., Q Liu, *Experimental Investigation of Surfactant ADsorption on Sand and Oil-Water Interface in Heavy Oil/Water/Sand Systems.* Petroleum Society Journals, 2005.
15. Mazen Ahmed Muherei, R.j., *Equilibrium Adsorption Isotherms of Anionic, Nonionic Surfactants and Their Mixtures to Shale and Sandstone.* Modern Applied Science, 2009. **3**(2).
16. Zargham Salari, M.A.A., Riaz Ahmadi, Riaz Kharrat, Abbas Abbaszadeh Shahri, *Experimental Studies of Cationic Surfactant Adsorption onto Carbonate Rocks.* Australian Journal of Basic and Applied Sciences, 2011. **5**(12): p. 808-813.
17. Hower, W.F., *Adsorption of Surfactants on Montmorillonite.* Clays and Clay Minerals, 1970. **18**: p. 97-105.
18. Krister Holmberg, B.J., Bengt Kronberg and Björn Lindman, *Surfactants and Polymers in Aqueous Solution*

2002(second edition): p. 357-387.

19. Krister Holmberg, B.J., Bengt Kronberg and Björn Lindman, *Surfactants and Polymers in Aqueous Solution*

2002(second edition): p. 337-355.

20. Mørk, P.C., *Overflate og Kolloidkjemi.* 2004. **8th edition**: p. 48-80.
21. Krister Holmberg, B.J., Bengt Kronberg and Björn Lindman, *Surfactants and Polymers in Aqueous Solution.* 2002. **Second Edition**: p. 10.
22. Schramm, L.L., *Surfactants: Fundamentals and Application in the Petroleum Industry.* 2000: p. 3-51.
23. Krister Holmberg, B.J., Bengt Kronberg and Björn Lindman, *Surfactants and Polymers in Aqueous Solution.* 2002. **Second Edition**: p. 1-36

24. Krister Holmberg, B.J., Bengt Kronberg and Björn Lindman, *Surfactants and Polymers in Aqueous Solution.* 2002. **Second Edition**: p. 39-66.
25. Krister Holmberg, B.J., Bengt Kronberg and Björn Lindman, *Surfactants and Polymers in Aqueous Solution.* 2002. **Second edition**.
26. Krister Holmberg, B.J., Bengt Kronberg and Björn Lindman, *Surfactants and Polymers in Aqueous Solution*

2002(second edition): p. 90.

27. Krister Holmberg, B.J., Bengt Kronberg and Björn Lindman, *Surfactants and Polymers in Aqueous Solution.* 2002. **Second Edition**: p. 344

28. Krister Holmberg, B.J., Bengt Kronberg and Björn Lindman, *Surfactants and Polymers in Aqueous Solution.* 2002. **Second Edition**: p. 358

29. Krister Holmberg, B.J., Bengt Kronberg and Björn Lindman, *Surfactants and Polymers in Aqueous Solution*

2002(second edition): p. 363.

30. Schramm, L.L., *Surfactants: Fundamentals and Application in the Petroleum Industry.* 2000: p. 179.
31. Schramm, L.L., *Surfactants: Fundamentals and Application in the Petroleum Industry.* 2000: p. 129.
32. instruments, M., *Zetasizer Nano Manual, Techincal note, Code: MRK654-01.*
33. Mørk, P.C., *Overflate og Kolloidkjemi.* 2004. **8th edition**: p. 194-212.
34. Jun Kameda, K.S., Daniel Beaufort, Toshohiro Kogure, *Textures and polytypes in vermiform kaolins diagenetically formed in a sandstone reservoir: a FIB-TEM investigation.* European Journal of Mineralogy, 2008. **20**: p. 199-204.
35. Etelka Tomácz, M.S., *Surface charge heterogenity of kaolinite in aqueous suspension on comparison with montmorilloninte.* Applied Clay Science, 2006. **34**(1-4): p. 105-124.
36. instruments, M., *Zetasizer Nano Manual, Techincal note, Code: MRK669-01.*
37. SIGMA, K., *Sigma 71 Instructional Manual.* 2001.

7 List of Appendices

A – Risk Assessment

B – Adsorption data: Low salinity, 6x series

C – Adsorption data: Low salinity, 9x series

D – Adsorption data: Low salinity with calcium, 8x series

E – Adsorption data: High salinity, 5x series

F – Adsorption data: High salinity with calcium, 7x series

G – Adsorption data: High salinity, 4x series

H – Adsorption data: Calculation of salinities

I – Change in pH over 36 hours.

Appendix A: Risk assessment

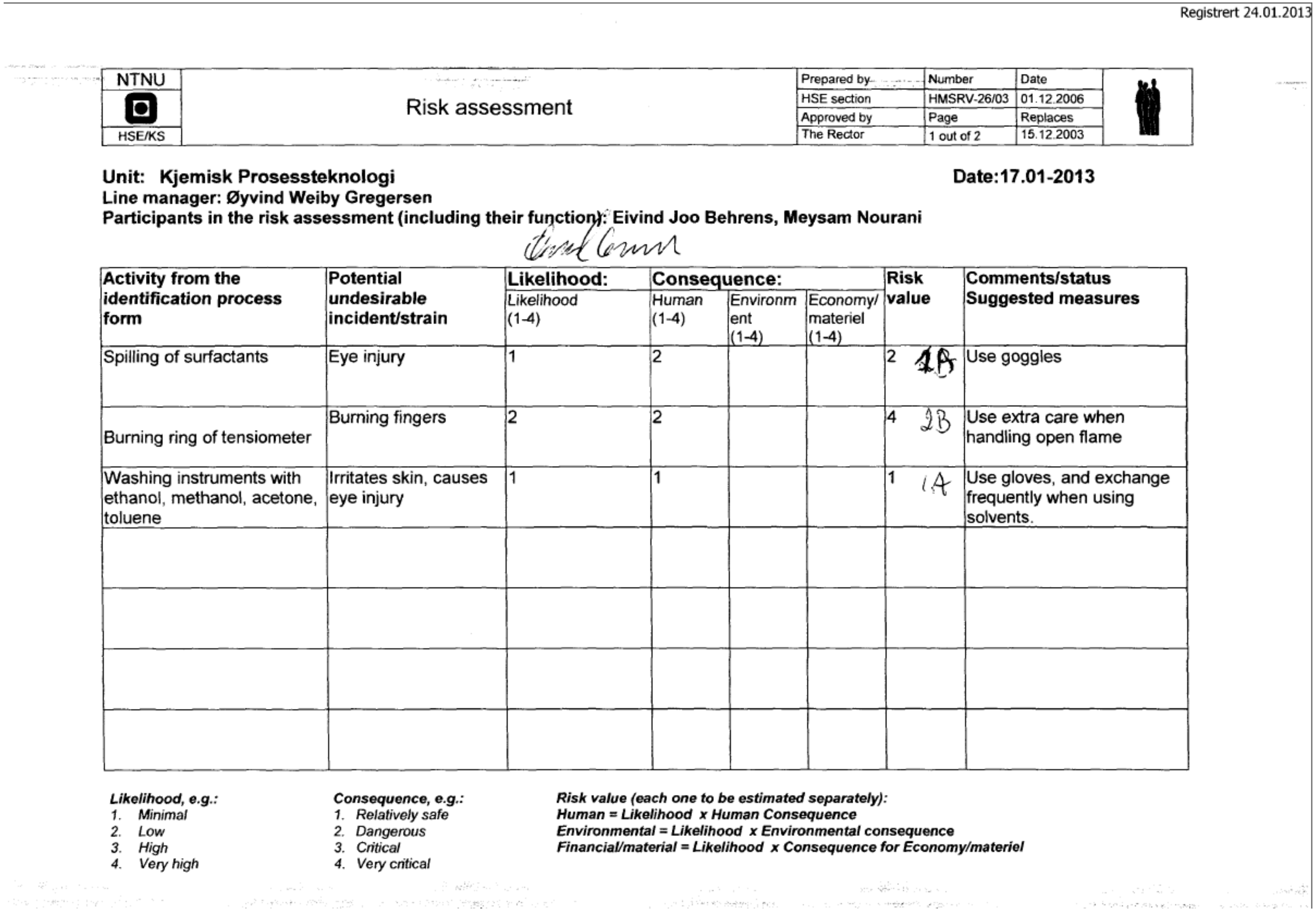

Registrert 24.01.2013

NTNU	Risk assessment	Prepared by	Number	Date
		HSE section	HMSRV-26/03	01.12.2006
		Approved by	Page	Replaces
HSE/KS		The Rector	1 out of 2	15.12.2003

Unit: Kjemisk Prosessteknologi **Date:17.01-2013**
Line manager: Øyvind Weiby Gregersen
Participants in the risk assessment (including their function): Eivind Joo Behrens, Meysam Nourani

Activity from the identification process form	**Potential undesirable incident/strain**	**Likelihood:**	**Consequence:**			**Risk value**	**Comments/status Suggested measures**
		Likelihood (1-4)	Human (1-4)	Environment (1-4)	Economy/ materiel (1-4)		
Spilling of surfactants	Eye injury	1	2			2 1B	Use goggles
Burning ring of tensiometer	Burning fingers	2	2			4 2B	Use extra care when handling open flame
Washing instruments with ethanol, methanol, acetone, toluene	Irritates skin, causes eye injury	1	1			1 1A	Use gloves, and exchange frequently when using solvents.

Likelihood, e.g.:
1. *Minimal*
2. *Low*
3. *High*
4. *Very high*

Consequence, e.g.:
1. *Relatively safe*
2. *Dangerous*
3. *Critical*
4. *Very critical*

Risk value (each one to be estimated separately):
Human = Likelihood x Human Consequence
Environmental = Likelihood x Environmental consequence
Financial/material = Likelihood x Consequence for Economy/materiel

Appendix A: Risk assessment

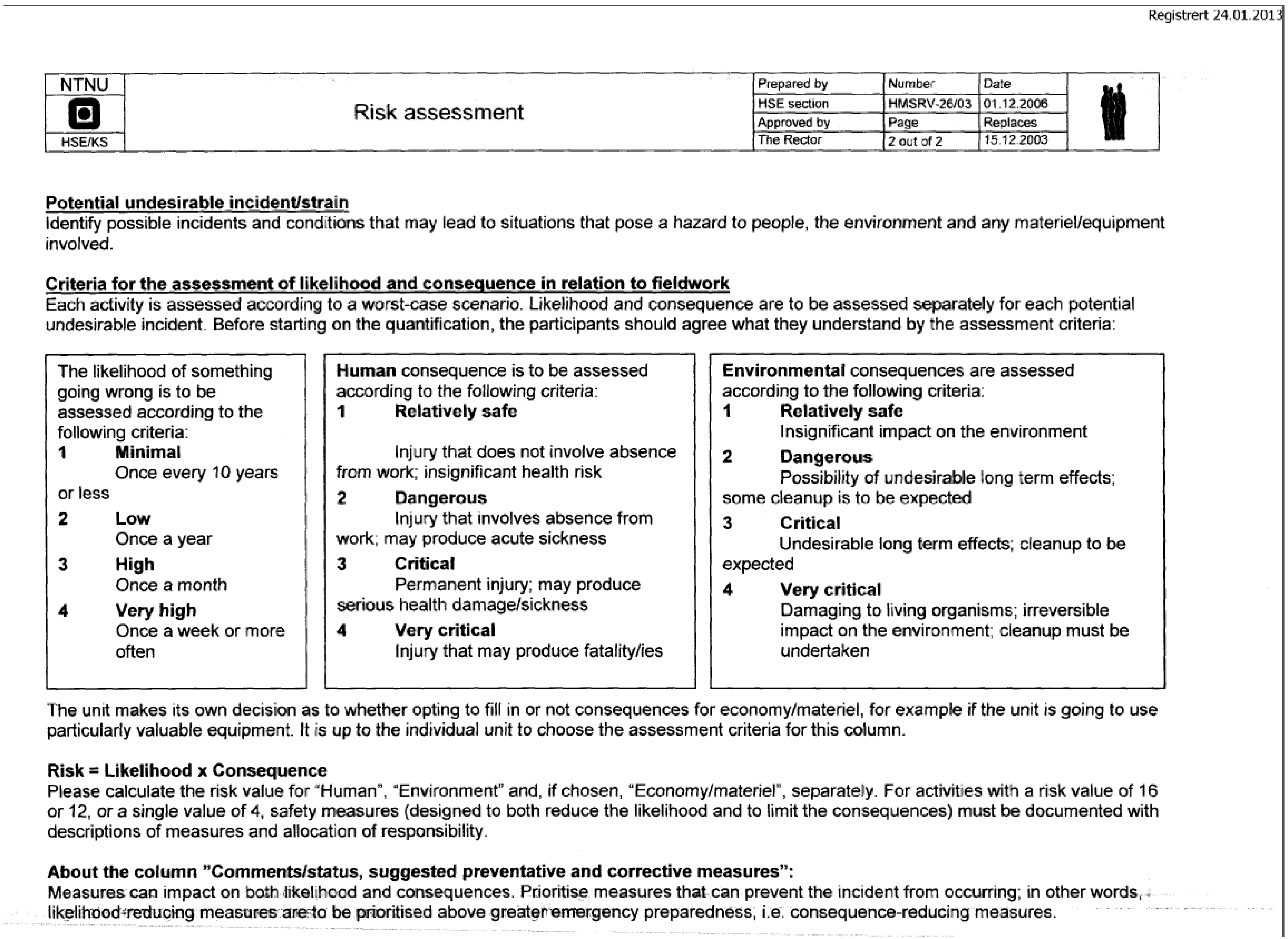

Registrert 24.01.2013

NTNU	Risk assessment	Prepared by	Number	Date
HSE/KS		HSE section	HMSRV-26/03	01.12.2006
		Approved by	Page	Replaces
		The Rector	2 out of 2	15.12.2003

Potential undesirable incident/strain

Identify possible incidents and conditions that may lead to situations that pose a hazard to people, the environment and any materiel/equipment involved.

Criteria for the assessment of likelihood and consequence in relation to fieldwork

Each activity is assessed according to a worst-case scenario. Likelihood and consequence are to be assessed separately for each potential undesirable incident. Before starting on the quantification, the participants should agree what they understand by the assessment criteria:

The likelihood of something going wrong is to be assessed according to the following criteria:

1 **Minimal**
Once every 10 years or less

2 **Low**
Once a year

3 **High**
Once a month

4 **Very high**
Once a week or more often

Human consequence is to be assessed according to the following criteria:

1 **Relatively safe**
Injury that does not involve absence from work; insignificant health risk

2 **Dangerous**
Injury that involves absence from work; may produce acute sickness

3 **Critical**
Permanent injury; may produce serious health damage/sickness

4 **Very critical**
Injury that may produce fatality/ies

Environmental consequences are assessed according to the following criteria:

1 **Relatively safe**
Insignificant impact on the environment

2 **Dangerous**
Possibility of undesirable long term effects; some cleanup is to be expected

3 **Critical**
Undesirable long term effects; cleanup to be expected

4 **Very critical**
Damaging to living organisms; irreversible impact on the environment; cleanup must be undertaken

The unit makes its own decision as to whether opting to fill in or not consequences for economy/materiel, for example if the unit is going to use particularly valuable equipment. It is up to the individual unit to choose the assessment criteria for this column.

Risk = Likelihood x Consequence

Please calculate the risk value for "Human", "Environment" and, if chosen, "Economy/materiel", separately. For activities with a risk value of 16 or 12, or a single value of 4, safety measures (designed to both reduce the likelihood and to limit the consequences) must be documented with descriptions of measures and allocation of responsibility.

About the column "Comments/status, suggested preventative and corrective measures":

Measures can impact on both likelihood and consequences. Prioritise measures that can prevent the incident from occurring; in other words, likelihood-reducing measures are to be prioritised above greater emergency preparedness, i.e. consequence-reducing measures.

Appendix A: Risk assessment

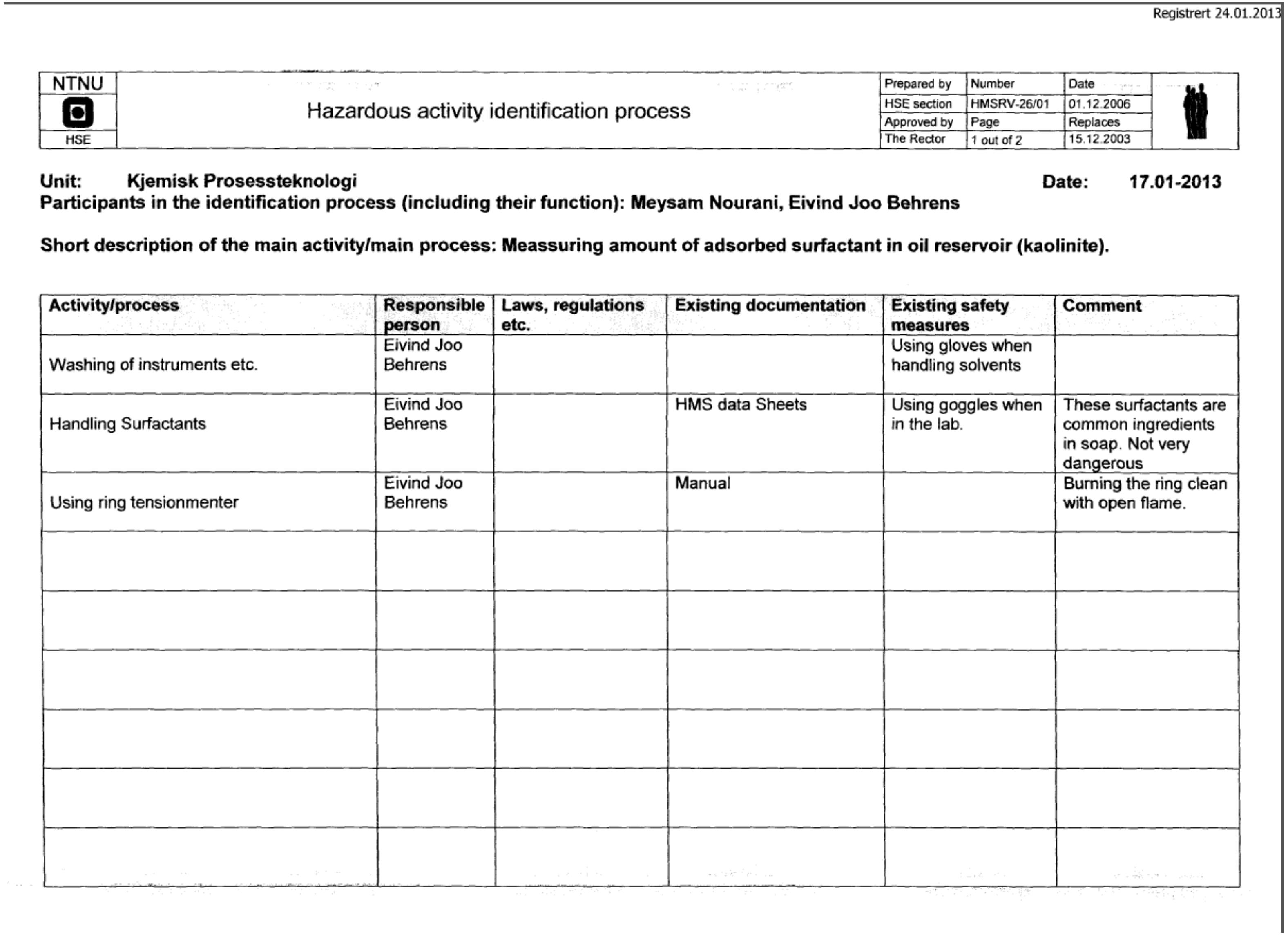

Registrert 24.01.2013

NTNU HSE	Hazardous activity identification process	Prepared by HSE section	Number HMSRV-26/01	Date 01.12.2006
		Approved by The Rector	Page 1 out of 2	Replaces 15.12.2003

Unit: **Kjemisk Prosessteknologi** **Date:** **17.01-2013**

Participants in the identification process (including their function): Meysam Nourani, Eivind Joo Behrens

Short description of the main activity/main process: Meassuring amount of adsorbed surfactant in oil reservoir (kaolinite).

Activity/process	**Responsible person**	**Laws, regulations etc.**	**Existing documentation**	**Existing safety measures**	**Comment**
Washing of instruments etc.	Eivind Joo Behrens			Using gloves when handling solvents	
Handling Surfactants	Eivind Joo Behrens		HMS data Sheets	Using goggles when in the lab.	These surfactants are common ingredients in soap. Not very dangerous
Using ring tensionmenter	Eivind Joo Behrens		Manual		Burning the ring clean with open flame.

Appendix B: adsorption data LoSal - #6x series.

Tensiometer data: Low Salinity measurements. #6x series:

IFT of #6x series LoSal								
		Time (minutes)						
Concentration		**Ref**	**5**	**30**	**60**	**240**	**480**	**1440**
10^-3 M	**# 61**	26,630	25,817	25,752	25,757	25,775	25,748	25,709
5*10^-4 M	**# 62**	30,471	29,621	29,630	29,568	29,581	29,549	29,610
10^-4 M	**# 62**	38,823	39,005	39,090	39,026	39,168	39,258	39,052
5*10^-5 M	**# 64**	42,287	43,077	43,074	42,823	42,802	42,728	42,848
10^-5 M	**# 65**	50,690	51,911	51,996	51,856	52,081	52,241	52,522

Equation describing IFT as a function of surfactant concentration:

Formula, LoSal:	Y=-5,69*ln(x)-12,73	solved for X:	X= e^((y/-5,69)-(12,73/5,69))
Y:	IFT		
X:	Concentration		

Calculated Surfactant concentration based on the describing equation:

Concentration								
		Time (minutes)						
Concentration		**Ref**	**5**	**30**	**60**	**240**	**480**	**1440**
10^-3 M	**# 61**	9,90E-04	1,14E-03	1,16E-03	1,15E-03	1,15E-03	1,16E-03	1,16E-03
5*10^-4 M	**# 62**	5,04E-04	5,86E-04	5,85E-04	5,91E-04	5,90E-04	5,93E-04	5,87E-04
10^-4 M	**# 62**	1,16E-04	1,13E-04	1,11E-04	1,12E-04	1,09E-04	1,08E-04	1,12E-04
5*10^-5 M	**# 64**	6,32E-05	5,50E-05	5,50E-05	5,75E-05	5,77E-05	5,85E-05	5,73E-05
10^-5 M	**# 65**	1,44E-05	1,16E-05	1,15E-05	1,18E-05	1,13E-05	1,10E-05	1,05E-05

Calculated amount of adsorbed surfactant, concentration subtracted from the reference value

Difference in Concentration, Adsorbance [M]

		Time (minutes)						
Concentration		**Ref**	**5**	**30**	**60**	**240**	**480**	**1440**
10^-3 M	**# 61**	0	-1,52E-04	-1,65E-04	-1,64E-04	-1,61E-04	-1,66E-04	-1,74E-04
5*10^-4 M	**# 62**	0	-8,13E-05	-8,03E-05	-8,67E-05	-8,54E-05	-8,87E-05	-8,24E-05
10^-4 M	**# 62**	0	3,65E-06	5,32E-06	4,08E-06	6,84E-06	8,55E-06	4,58E-06
5*10^-5 M	**# 64**	0	8,19E-06	8,17E-06	5,69E-06	5,47E-06	4,72E-06	5,94E-06
10^-5 M	**# 65**	0	2,79E-06	2,96E-06	2,67E-06	3,13E-06	3,44E-06	3,97E-06

Recalculated: g. surfactant per liter of solution

Adsorbed amount, [g/l]

		Time (minutes)						
Concentration		Ref	5	30	60	240	480	1440
10^-3 M	# 61	0	-0,068	-0,073	-0,073	-0,071	-0,074	-0,077
5*10^-4 M	# 62	0	-0,036	-0,036	-0,039	-0,038	-0,039	-0,037
10^-4 M	# 62	0	0,002	0,002	0,002	0,003	0,004	0,002
5*10^-5 M	# 64	0	0,004	0,004	0,003	0,002	0,002	0,003
10^-5 M	# 65	0	0,001	0,001	0,001	0,001	0,002	0,002

Recalculated g. surfactant per batch (30ml)

Adsorbed amount, [g/batch]

		Time (minutes)						
Concentration		**Ref**	**5**	**30**	**60**	**240**	**480**	**1440**
10^-3 M	**# 61**	0	-2,03E-03	-2,20E-03	-2,19E-03	-2,14E-03	-2,21E-03	-2,32E-03
5*10^-4 M	**# 62**	0	-1,08E-03	-1,07E-03	-1,16E-03	-1,14E-03	-1,18E-03	-1,10E-03
10^-4 M	**# 62**	0	4,87E-05	7,08E-05	5,43E-05	9,11E-05	1,14E-04	6,10E-05
5*10^-5 M	**# 64**	0	1,09E-04	1,09E-04	7,57E-05	7,29E-05	6,29E-05	7,91E-05
10^-5 M	**# 65**	0	3,71E-05	3,94E-05	3,56E-05	4,17E-05	4,59E-05	5,29E-05

Recalculated: g. surfactant per g. kaolinite (0,3g per batch):

Adsorbed amount, [g surf adsorbed/g kaolinite]								
		Time (minutes)						
Concentration		**Ref**	**5**	**30**	**60**	**240**	**480**	**1440**
10^-3 M	**# 61**	0	-6,75E-03	-7,34E-03	-7,29E-03	-7,13E-03	-7,37E-03	-7,73E-03
5*10^-4 M	**# 62**	0	-3,61E-03	-3,57E-03	-3,85E-03	-3,79E-03	-3,94E-03	-3,66E-03
10^-4 M	**# 62**	0	1,62E-04	2,36E-04	1,81E-04	3,04E-04	3,80E-04	2,03E-04
5*10^-5 M	**# 64**	0	3,64E-04	3,63E-04	2,52E-04	2,43E-04	2,10E-04	2,64E-04
10^-5 M	**# 65**	0	1,24E-04	1,31E-04	1,19E-04	1,39E-04	1,53E-04	1,76E-04

Appendix C: adsorption data LoSal - #9x series.

Tensiometer data: Low Salinity measurements 9x series:

IFT of #9x series LoSal								
		Time (minutes)						
Concentration		**Ref**	**5**	**30**	**60**	**240**	**440**	**1440**
10^-3 M	**# 91**	26,7	25,71	25,84	25,65	25,67	25,62	25,76
5*10^-4 M	**# 92**	28,51	27,54	27,45	27,66	27,706	27,6	27,57
10^-4 M	**# 92**	39,87	39,29	39,25	39,32	39,35	39,35	39,29
5*10^-5 M	**# 94**	41,59	41,22	41,18	41,33	41,34	41,21	41,2
10^-5 M	**# 95**	52,5	52,17	52,23	52,55	52,45	52,62	52,55

Equation describing IFT as a function of surfactant concentration:

Formula, LoSal:	Y=-5,69*ln(x)-12,73	solved for X:	X= e^((y/-5,69)-(12,73/5,69))
Y:	IFT		
X:	Concentration		

Calculated Surfactant concentration based on the describing equation:

Concentration								
		Time (minutes)						
Concentration		**Ref**	**5**	**30**	**60**	**240**	**480**	**1440**
10^-3 M	**# 91**	9,78E-04	1,16E-03	1,14E-03	1,18E-03	1,17E-03	1,18E-03	1,15E-03
5*10^-4 M	**# 92**	7,12E-04	8,44E-04	8,57E-04	8,26E-04	8,20E-04	8,35E-04	8,40E-04
10^-4 M	**# 92**	9,67E-05	1,07E-04	1,08E-04	1,06E-04	1,06E-04	1,06E-04	1,07E-04
5*10^-5 M	**# 94**	7,14E-05	7,62E-05	7,68E-05	7,48E-05	7,47E-05	7,64E-05	7,65E-05
10^-5 M	**# 95**	1,05E-05	1,11E-05	1,10E-05	1,04E-05	1,06E-05	1,03E-05	1,04E-05

Calculated amount of adsorbed surfactant, concentration subtracted from the reference value:

Difference in Concentration, Adsorbance [M]

		Time (minutes)						
Concentration		**Ref**	**5**	**30**	**60**	**240**	**480**	**1440**
10^-3 M	**# 91**	0	-1,86E-04	-1,60E-04	-1,98E-04	-1,94E-04	-2,04E-04	-1,76E-04
5*10^-4 M	**# 92**	0	-1,32E-04	-1,46E-04	-1,15E-04	-1,08E-04	-1,23E-04	-1,28E-04
10^-4 M	**# 92**	0	-1,04E-05	-1,11E-05	-9,81E-06	-9,25E-06	-9,25E-06	-1,04E-05
5*10^-5 M	**# 94**	0	-4,80E-06	-5,34E-06	-3,34E-06	-3,21E-06	-4,93E-06	-5,07E-06
10^-5 M	**# 95**	0	-6,27E-07	-5,10E-07	9,19E-08	-9,27E-08	2,19E-07	9,19E-08

Recalculated: g. surfactant per liter of solution:

Adsorbed amount, [g/l]

		Time (minutes)						
Concentration		**Ref**	**5**	**30**	**60**	**240**	**480**	**1440**
10^-3 M	**# 91**	0	-8,25E-02	-7,09E-02	-8,80E-02	-8,62E-02	-9,08E-02	-7,80E-02
5*10^-4 M	**# 92**	0	-5,87E-02	-6,47E-02	-5,09E-02	-4,80E-02	-5,48E-02	-5,68E-02
10^-4 M	**# 92**	0	-4,61E-03	-4,94E-03	-4,36E-03	-4,11E-03	-4,11E-03	-4,61E-03
5*10^-5 M	**# 94**	0	-2,13E-03	-2,37E-03	-1,48E-03	-1,42E-03	-2,19E-03	-2,25E-03
10^-5 M	**# 95**	0	-2,78E-04	-2,27E-04	4,08E-05	-4,12E-05	9,73E-05	4,08E-05

Recalculated: g surfactant per batch (30 ml)

Adsorbed amount, [g/batch]

		Time (minutes)						
Concentration		**Ref**	**5**	**30**	**60**	**240**	**480**	**1440**
10^-3 M	**# 91**	0	-2,48E-03	-2,13E-03	-2,64E-03	-2,59E-03	-2,72E-03	-2,34E-03
5*10^-4 M	**# 92**	0	-1,76E-03	-1,94E-03	-1,53E-03	-1,44E-03	-1,64E-03	-1,70E-03
10^-4 M	**# 92**	0	-1,38E-04	-1,48E-04	-1,31E-04	-1,23E-04	-1,23E-04	-1,38E-04
5*10^-5 M	**# 94**	0	-6,39E-05	-7,11E-05	-4,45E-05	-4,27E-05	-6,57E-05	-6,75E-05
10^-5 M	**# 95**	0	-8,35E-06	-6,80E-06	1,22E-06	-1,23E-06	2,92E-06	1,22E-06

Recalculated: g. surfactant per g. kaolinite (0,3g per batch)

Adsorbed amount, [g surf adsorbed/g kaolinite]

		Time (minutes)						
Concentration		**Ref**	**5**	**30**	**60**	**240**	**480**	**1440**
10^-3 M	**# 91**	0	-8,25E-03	-7,09E-03	-8,80E-03	-8,62E-03	-9,08E-03	-7,80E-03
5*10^-4 M	**# 92**	0	-5,87E-03	-6,47E-03	-5,09E-03	-4,80E-03	-5,48E-03	-5,68E-03
10^-4 M	**# 92**	0	-4,61E-04	-4,94E-04	-4,36E-04	-4,11E-04	-4,11E-04	-4,61E-04
5*10^-5 M	**# 94**	0	-2,13E-04	-2,37E-04	-1,48E-04	-1,42E-04	-2,19E-04	-2,25E-04
10^-5 M	**# 95**	0	-2,78E-05	-2,27E-05	4,08E-06	-4,12E-06	9,73E-06	4,08E-06

Appendix D: adsorption data LoSal w. cal. – #8x series.

Tensiometer data: Low Salinity with calcium measurements, 8x series

IFT of #8x series LoSal with calcium

		Time (minutes)						
Concentration		**Ref**	**5**	**30**	**60**	**240**	**480**	**1440**
10^-3 M	**# 81**	25,481	25,455	25,520	25,481	25,468	25,468	25,500
5*10^-4 M	**# 82**	26,648	27,349	27,304	27,291	27,348	27,322	27,311
10^-4 M	**# 83**	34,199	34,843	35,007	34,976	34,919	34,947	35,031
5*10^-5 M	**# 84**	39,807	41,024	41,096	41,132	41,218	41,038	41,122
10^-5 M	**# 85**	49,362	50,533	50,411	50,529	50,386	50,361	50,557

Equation describing IFT as a function of surfactant concentration:

Formula, LoSal with calsium:	Y=-5,18*ln(x)-11,6	solved for X:	X= e^((y/-5,18)-(11,6/5,18))
Y:	IFT		
X:	Concentration		

Calculated Surfactant concentration based on the describing equation:

Concentration

		Time (minutes)						
Concentration		**Ref**	**5**	**30**	**60**	**240**	**480**	**1440**
10^-3 M	**# 81**	7,78E-04	7,82E-04	7,72E-04	7,78E-04	7,80E-04	7,80E-04	7,75E-04
5*10^-4 M	**# 82**	6,21E-04	5,43E-04	5,47E-04	5,49E-04	5,43E-04	5,45E-04	5,47E-04
10^-4 M	**# 83**	1,45E-04	1,28E-04	1,24E-04	1,24E-04	1,26E-04	1,25E-04	1,23E-04
5*10^-5 M	**# 84**	4,90E-05	3,87E-05	3,82E-05	3,79E-05	3,73E-05	3,86E-05	3,80E-05
10^-5 M	**# 85**	7,74E-06	6,18E-06	6,32E-06	6,18E-06	6,35E-06	6,38E-06	6,15E-06

Calculated amount of adsorbed surfactant, concentration subtracted from the reference value:

Concentration

		Time (minutes)						
Concentration		**Ref**	**5**	**30**	**60**	**240**	**480**	**1440**
10^-3 M	**# 81**	7,78E-04	7,82E-04	7,72E-04	7,78E-04	7,80E-04	7,80E-04	7,75E-04
5*10^-4 M	**# 82**	6,21E-04	5,43E-04	5,47E-04	5,49E-04	5,43E-04	5,45E-04	5,47E-04
10^-4 M	**# 83**	1,45E-04	1,28E-04	1,24E-04	1,24E-04	1,26E-04	1,25E-04	1,23E-04
5*10^-5 M	**# 84**	4,90E-05	3,87E-05	3,82E-05	3,79E-05	3,73E-05	3,86E-05	3,80E-05
10^-5 M	**# 85**	7,74E-06	6,18E-06	6,32E-06	6,18E-06	6,35E-06	6,38E-06	6,15E-06

Recalculated: g surfactant per liter of solution:

Adsorbed amount, [g/l]

		Time (minutes)						
Concentration		**Ref**	**5**	**30**	**60**	**240**	**480**	**1440**
10^-3 M	**# 81**	0	-1,74E-03	2,59E-03	0,00E+00	-8,68E-04	-8,68E-04	1,27E-03
5*10^-4 M	**# 82**	0	3,49E-02	3,28E-02	3,22E-02	3,48E-02	3,37E-02	3,31E-02
10^-4 M	**# 83**	0	7,51E-03	9,28E-03	8,94E-03	8,33E-03	8,64E-03	9,53E-03
5*10^-5 M	**# 84**	0	4,55E-03	4,79E-03	4,91E-03	5,19E-03	4,60E-03	4,88E-03
10^-5 M	**# 85**	0	6,96E-04	6,30E-04	6,93E-04	6,17E-04	6,03E-04	7,08E-04

Recalculated: g surfactant per batch (30ml):

Adsorbed amount, [g/batch]

		Time (minutes)						
Concentration		**Ref**	**5**	**30**	**60**	**240**	**480**	**1440**
10^-3 M	**# 81**	0	-5,22E-05	7,78E-05	0,00E+00	-2,60E-05	-2,60E-05	3,80E-05
5*10^-4 M	**# 82**	0	1,05E-03	9,84E-04	9,65E-04	1,04E-03	1,01E-03	9,93E-04
10^-4 M	**# 83**	0	2,25E-04	2,78E-04	2,68E-04	2,50E-04	2,59E-04	2,86E-04
5*10^-5 M	**# 84**	0	1,37E-04	1,44E-04	1,47E-04	1,56E-04	1,38E-04	1,46E-04
10^-5 M	**# 85**	0	2,09E-05	1,89E-05	2,08E-05	1,85E-05	1,81E-05	2,12E-05

Recalculated: g. surfactant per g. kaolinite (0,3g per batch)

Adsorbed amount, [g surf adsorbed/g kaolinite]

		Time (minutes)						
Concentration		**Ref**	**5**	**30**	**60**	**240**	**480**	**1440**
10^-3 M	# 81	0	-1,74E-04	2,59E-04	0,00E+00	-8,68E-05	-8,68E-05	1,27E-04
5*10^-4 M	# 82	0	3,49E-03	3,28E-03	3,22E-03	3,48E-03	3,37E-03	3,31E-03
10^-4 M	# 83	0	7,51E-04	9,28E-04	8,94E-04	8,33E-04	8,64E-04	9,53E-04
5*10^-5 M	# 84	0	4,55E-04	4,79E-04	4,91E-04	5,19E-04	4,60E-04	4,88E-04
10^-5 M	# 85	0	6,96E-05	6,30E-05	6,93E-05	6,17E-05	6,03E-05	7,08E-05

Appendid E: adsorption data HiSal - #5x series.

Tensiometer data: High salinity measurements, 5x series:

IFT of #5x series HiSal								
		Time (minutes)						
Concentration		**Ref**	**5**	**30**	**60**	**240**	**480**	**1440**
5*10^-5 M	# 51	26,607	28,636	28,711	28,831	28,572	28,846	29,003
10^-5 M	# 52	37,287	38,728	38,835	38,793	39,174	39,068	39,023
5*10^-6 M	# 52	42,337	43,801	44,830	45,041	45,530	45,942	46,082
10^-6 M	# 54	53,438	58,418	58,921	59,476	59,959	59,440	59,795
5*10^-7 M	# 55	56,718	61,211	62,424	63,221	56,762	63,422	63,679

Equation describing IFT as a function of surfactant concentration

Formula, LoSal:	Y=-7,04*ln(x)-42,59	solved for X:	X= e^((y/-7,04)-(42,59/7,04))
Y:	IFT		
X:	Concentration		

Calculated Surfactant concentration based on the describing equation:

Concentration								
		Time (minutes)						
Concentration		**Ref**	**5**	**30**	**60**	**240**	**480**	**1440**
5*10^-5 M	**# 51**	5,39E-05	4,04E-05	3,99E-05	3,93E-05	4,07E-05	3,92E-05	3,83E-05
10^-5 M	**# 52**	1,18E-05	9,63E-06	9,48E-06	9,54E-06	9,04E-06	9,17E-06	9,23E-06
5*10^-6 M	**# 52**	5,77E-06	4,68E-06	4,05E-06	3,93E-06	3,66E-06	3,46E-06	3,39E-06
10^-6 M	**# 54**	1,19E-06	5,87E-07	5,47E-07	5,05E-07	4,72E-07	5,08E-07	4,83E-07
5*10^-7 M	**# 55**	7,48E-07	3,95E-07	3,32E-07	2,97E-07	7,43E-07	2,89E-07	2,78E-07

Calculated amount of adsorbed surfactant, concentration subtracted from the reference value:

Difference in Concentration, Adsorbance [M]

		Time (minutes)						
Concentration		**Ref**	**5**	**30**	**60**	**240**	**480**	**1440**
5*10^-5 M	**# 51**	0	1,35E-05	1,39E-05	1,46E-05	1,31E-05	1,47E-05	1,55E-05
10^-5 M	**# 52**	0	2,19E-06	2,33E-06	2,28E-06	2,78E-06	2,64E-06	2,58E-06
5*10^-6 M	**# 52**	0	1,08E-06	1,72E-06	1,84E-06	2,10E-06	2,31E-06	2,38E-06
10^-6 M	**# 54**	0	6,04E-07	6,45E-07	6,86E-07	7,20E-07	6,83E-07	7,08E-07
5*10^-7 M	**# 55**	0	3,53E-07	4,15E-07	4,51E-07	4,65E-09	4,59E-07	4,70E-07

Recalculated: g. surfactant per liter of solution:

Adsorbed amount, [g/l]

		Time (minutes)						
Concentration		**Ref**	**5**	**30**	**60**	**240**	**480**	**1440**
5*10^-5 M	**# 51**	0	5,99E-03	6,18E-03	6,48E-03	5,82E-03	6,51E-03	6,90E-03
10^-5 M	**# 52**	0	9,71E-04	1,04E-03	1,01E-03	1,23E-03	1,17E-03	1,15E-03
5*10^-6 M	**# 52**	0	4,81E-04	7,63E-04	8,16E-04	9,33E-04	1,03E-03	1,06E-03
10^-6 M	**# 54**	0	2,68E-04	2,86E-04	3,05E-04	3,19E-04	3,03E-04	3,15E-04
5*10^-7 M	**# 55**	0	1,57E-04	1,84E-04	2,00E-04	2,06E-06	2,04E-04	2,08E-04

Recalculated: g. surfactant per batch (30ml):

Adsorbed amount, [g/batch]

		Time (minutes)						
Concentration		**Ref**	**0**	**5,5**	**12**	**17**	**28**	**75**
5*10^-5 M	**# 51**	0	1,80E-04	1,85E-04	1,94E-04	1,75E-04	1,95E-04	2,07E-04
10^-5 M	**# 52**	0	2,91E-05	3,11E-05	3,03E-05	3,70E-05	3,52E-05	3,44E-05
5*10^-6 M	**# 52**	0	1,44E-05	2,29E-05	2,45E-05	2,80E-05	3,08E-05	3,17E-05
10^-6 M	**# 54**	0	8,05E-06	8,59E-06	9,14E-06	9,58E-06	9,10E-06	9,44E-06
5*10^-7 M	**# 55**	0	4,70E-06	5,53E-06	6,01E-06	6,19E-08	6,12E-06	6,25E-06

Recalculated: g. surfactant per g. kaolinite (0,3g per batch):

Adsorbed amount, [g surf adsorbed/g kaolinite]								
		Time (minutes)						
Concentration		**Ref**	**5**	**30**	**60**	**240**	**480**	**1440**
5*10^-5 M	**# 51**	0	5,99E-04	6,18E-04	6,48E-04	5,82E-04	6,51E-04	6,90E-04
10^-5 M	**# 52**	0	9,71E-05	1,04E-04	1,01E-04	1,23E-04	1,17E-04	1,15E-04
5*10^-6 M	**# 52**	0	4,81E-05	7,63E-05	8,16E-05	9,33E-05	1,03E-04	1,06E-04
10^-6 M	**# 54**	0	2,68E-05	2,86E-05	3,05E-05	3,19E-05	3,03E-05	3,15E-05
5*10^-7 M	**# 55**	0	1,57E-05	1,84E-05	2,00E-05	2,06E-07	2,04E-05	2,08E-05

Appendix F: adsorption data HiSal w. cal. - #7x series

Tensiometer data: High salinity with calcium measurements, 9x series:

IFT of #7x series HiSal.Cal								
		Time (minutes)						
Consentration		**Ref**	**5**	**30**	**60**	**240**	**480**	**1440**
5*10^-5 M	**# 71**	26,800	29,056	29,389	29,398	29,440	29,530	29,680
10^-5 M	**# 72**	37,160	39,110	39,130	39,260	39,780	39,540	40,200
5*10^-6 M	**# 73**	42,580	47,620	47,150	47,570	47,930	45,680	47,530
10^-6 M	**# 74**	56,010	62,710	61,590	61,940	62,120	63,390	62,800
5*10^-7 M	**# 75**	59,576	64,740	71,620	68,530	68,450	71,170	68,810

Equation describing IFT as a function of surfactant concentration:

Formula, LoSal:	Y=-7,39*ln(x)-46,07	solved for X:	X= e^((y/-7,39)-(46,07/7,39))
Y:	IFT		
X:	Concentration		

Calculated Surfactant concentration based on the describing equation:

Concentration								
		Time (minutes)						
Concentration		**Ref**	**5**	**30**	**60**	**240**	**480**	**1440**
5*10^-5 M	**# 71**	5,22E-05	3,85E-05	3,68E-05	3,67E-05	3,65E-05	3,61E-05	3,53E-05
10^-5 M	**# 72**	1,28E-05	9,87E-06	9,84E-06	9,67E-06	9,01E-06	9,31E-06	8,51E-06
5*10^-6 M	**# 73**	6,17E-06	3,12E-06	3,32E-06	3,14E-06	2,99E-06	4,06E-06	3,16E-06
10^-6 M	**# 74**	1,00E-06	4,05E-07	4,71E-07	4,49E-07	4,38E-07	3,69E-07	4,00E-07
5*10^-7 M	**# 75**	6,19E-07	3,08E-07	1,21E-07	1,84E-07	1,86E-07	1,29E-07	1,77E-07

Calculated amount of adsorbed surfactant, concentration subtracted from the reference value:

Difference in Concentration, Adsorbance [M]

		Time (minutes)						
Concentration		**Ref**	**5**	**30**	**60**	**240**	**480**	**1440**
5*10^-5 M	**# 71**	0	1,37E-05	1,54E-05	1,55E-05	1,57E-05	1,61E-05	1,68E-05
10^-5 M	**# 72**	0	2,98E-06	3,01E-06	3,18E-06	3,83E-06	3,54E-06	4,33E-06
5*10^-6 M	**# 73**	0	3,05E-06	2,85E-06	3,03E-06	3,18E-06	2,11E-06	3,01E-06
10^-6 M	**# 74**	0	5,97E-07	5,31E-07	5,53E-07	5,64E-07	6,33E-07	6,02E-07
5*10^-7 M	**# 75**	0	3,11E-07	4,97E-07	4,34E-07	4,32E-07	4,90E-07	4,41E-07

Recalculated: g. surfactant per liter of solution:

Adsorbed amount, [g/l]

		Time (minutes)						
Concentration		**Ref**	**5**	**30**	**60**	**240**	**480**	**1440**
5*10^-5 M	**# 71**	0	6,10E-03	6,85E-03	6,87E-03	6,96E-03	7,16E-03	7,48E-03
10^-5 M	**# 72**	0	1,32E-03	1,33E-03	1,41E-03	1,70E-03	1,57E-03	1,92E-03
5*10^-6 M	**# 73**	0	1,35E-03	1,26E-03	1,34E-03	1,41E-03	9,38E-04	1,34E-03
10^-6 M	**# 74**	0	2,65E-04	2,36E-04	2,46E-04	2,50E-04	2,81E-04	2,67E-04
5*10^-7 M	**# 75**	0	1,38E-04	2,21E-04	1,93E-04	1,92E-04	2,17E-04	1,96E-04

Recalculated: g. surfactant per batch (30ml):

Adsorbed amount, [g/batch]

		Time (minutes)						
Concentration		**Ref**	**5**	**30**	**60**	**240**	**480**	**1440**
5*10^-5 M	**# 71**	0	1,83E-04	2,05E-04	2,06E-04	2,09E-04	2,15E-04	2,24E-04
10^-5 M	**# 72**	0	3,97E-05	4,00E-05	4,23E-05	5,11E-05	4,71E-05	5,77E-05
5*10^-6 M	**# 73**	0	4,06E-05	3,79E-05	4,03E-05	4,23E-05	2,82E-05	4,01E-05
10^-6 M	**# 74**	0	7,96E-06	7,08E-06	7,37E-06	7,51E-06	8,43E-06	8,02E-06
5*10^-7 M	**# 75**	0	4,14E-06	6,62E-06	5,79E-06	5,76E-06	6,52E-06	5,88E-06

Recalculated : g. surfactant per g kaolinite (0,3g per batch):

Adsorbed amount, [g surf adsorbed/g kaolinite]

		Time (minutes)						
Concentration		**Ref**	**5**	**30**	**60**	**240**	**480**	**1440**
5*10^-5 M	**# 71**	0	6,10E-04	6,85E-04	6,87E-04	6,96E-04	7,16E-04	7,48E-04
10^-5 M	**# 72**	0	1,32E-04	1,33E-04	1,41E-04	1,70E-04	1,57E-04	1,92E-04
5*10^-6 M	**# 73**	0	1,35E-04	1,26E-04	1,34E-04	1,41E-04	9,38E-05	1,34E-04
10^-6 M	**# 74**	0	2,65E-05	2,36E-05	2,46E-05	2,50E-05	2,81E-05	2,67E-05
5*10^-7 M	**# 75**	0	1,38E-05	2,21E-05	1,93E-05	1,92E-05	2,17E-05	1,96E-05

Appendix G: adsorption data HiSal – #4x series.

Tensiometer data: High salinity measurements 4x series (not centrifuged)

IFT of #4x series HiSal

		Time (minutes)						
Concentration		**ref(0)**	**0**	**330**	**720**	**1020**	**1680**	**4500**
5*10^-5 M	**# 41**	27,370	28,650	29,204	29,273	29,240	29,300	29,306
10^-5 M	**# 42**	37,872	38,582	39,487	39,523	39,473	39,490	39,638
5*10^-6 M	**# 43**	42,851	43,834	45,751	45,887	46,004	45,952	45,825
10^-6 M	**# 44**	55,526	57,127	62,034	61,263	62,240	61,917	61,859
5*10^-7 M	**# 45**	59,210	59,713	68,052	66,633	67,697	67,605	66,667

Equation describing IFT as a function of surfactant concentration:

Formula, LoSal:	Y=-7,04*ln(x)-42,59	**solved for X**:	X= e^((y/-7,04)-(42,59/7,04))
Y:	**IFT**		
X:	**Concentration**		

Calculated surfactant concentration based on the describing equation:

Concentration

		Time (minutes)						
Concentration		**Ref**	**0**	**330**	**720**	**1020**	**1680**	**4500**
5*10^-5 M	**# 41**	4,83E-05	4,03E-05	3,72E-05	3,69E-05	3,71E-05	3,67E-05	3,67E-05
10^-5 M	**# 42**	1,09E-05	9,83E-06	8,64E-06	8,60E-06	8,66E-06	8,64E-06	8,46E-06
5*10^-6 M	**# 43**	5,36E-06	4,66E-06	3,55E-06	3,48E-06	3,43E-06	3,45E-06	3,51E-06
10^-6 M	**# 44**	8,86E-07	7,06E-07	3,51E-07	3,92E-07	3,41E-07	3,57E-07	3,60E-07
5*10^-7 M	**# 45**	5,25E-07	4,89E-07	1,49E-07	1,83E-07	1,57E-07	1,59E-07	1,82E-07

Calculated amount of adsorbed surfactant, concentration subtracted from the reference value:

Difference in Concentration, Adsorbance [M]

		Time (minutes)						
Concentration		**Ref**	**0**	**330**	**720**	**1020**	**1680**	**4500**
5*10^-5 M	**# 41**	0	8,04E-06	1,11E-05	1,14E-05	1,13E-05	1,16E-05	1,16E-05
10^-5 M	**# 42**	0	1,04E-06	2,23E-06	2,27E-06	2,21E-06	2,23E-06	2,41E-06
5*10^-6 M	**# 43**	0	6,99E-07	1,81E-06	1,88E-06	1,94E-06	1,91E-06	1,85E-06
10^-6 M	**# 44**	0	1,80E-07	5,34E-07	4,94E-07	5,44E-07	5,28E-07	5,25E-07
5*10^-7 M	**# 45**	0	3,62E-08	3,75E-07	3,42E-07	3,68E-07	3,66E-07	3,43E-07

Recalculated: g. surfactant per liter of solution:

Adsorbed amount, [g/l]

		Time (minutes)						
Concentration		**Ref**	**0**	**330**	**720**	**1020**	**1680**	**4500**
5*10^-5 M	**# 41**	0	3,57E-03	4,92E-03	5,08E-03	5,01E-03	5,15E-03	5,16E-03
10^-5 M	**# 42**	0	4,63E-04	9,90E-04	1,01E-03	9,82E-04	9,91E-04	1,07E-03
5*10^-6 M	**# 43**	0	3,10E-04	8,04E-04	8,34E-04	8,59E-04	8,48E-04	8,20E-04
10^-6 M	**# 44**	0	8,00E-05	2,37E-04	2,19E-04	2,42E-04	2,35E-04	2,33E-04
5*10^-7 M	**# 45**	0	1,61E-05	1,67E-04	1,52E-04	1,63E-04	1,62E-04	1,52E-04

Recalculated: g surfactant per batch (30ml)

Adsorbed amount, [g/batch]

		Time (minutes)						
Concentration		**Ref**	**0**	**330**	**720**	**1020**	**1680**	**4500**
5*10^-5 M	**# 41**	0	1,07E-04	1,48E-04	1,53E-04	1,50E-04	1,54E-04	1,55E-04
10^-5 M	**# 42**	0	1,39E-05	2,97E-05	3,03E-05	2,94E-05	2,97E-05	3,21E-05
5*10^-6 M	**# 43**	0	9,30E-06	2,41E-05	2,50E-05	2,58E-05	2,54E-05	2,46E-05
10^-6 M	**# 44**	0	2,40E-06	7,12E-06	6,58E-06	7,25E-06	7,04E-06	7,00E-06
5*10^-7 M	**# 45**	0	4,82E-07	5,00E-06	4,56E-06	4,90E-06	4,87E-06	4,57E-06

Recalculated: g surfactant per g. kaolinite (0,3g per batch):

Adsorbed amount, [g surf adsorbed/g kaolinite]								
		Time (minutes)						
Concentration		**Ref**	**0**	**330**	**720**	**1020**	**1680**	**4500**
5*10^-5 M	**# 41**	0	3,57E-04	4,92E-04	5,08E-04	5,01E-04	5,15E-04	5,16E-04
10^-5 M	**# 42**	0	4,63E-05	9,90E-05	1,01E-04	9,82E-05	9,91E-05	1,07E-04
5*10^-6 M	**# 43**	0	3,10E-05	8,04E-05	8,34E-05	8,59E-05	8,48E-05	8,20E-05
10^-6 M	**# 44**	0	8,00E-06	2,37E-05	2,19E-05	2,42E-05	2,35E-05	2,33E-05
5*10^-7 M	**# 45**	0	1,61E-06	1,67E-05	1,52E-05	1,63E-05	1,62E-05	1,52E-05

Appendix H: Calculation of Salinities

Ionic strength is given by the following equation:

$$I = \frac{1}{2}\sum_{i=1}^{n} C_i * z_i$$

Where *I* is the ionic strength, *z* is the charge of ion, and *c* is the molar concentration of that ion.

Low salinity solution:

Ionic strength of sample: 0,02

Ionic strength of solution: 0,04

$$0{,}04 = \frac{1}{2}[C_{NaCl} * (+1)^2 + C_{NaCl} * (-1)^2]$$

$$\boldsymbol{C_{NaCl} = 0,04\ M}$$

Low Salinity solution with calcium:

Ratio NaCl/CaCl2 = 1:45

Ionic strength of sample: 0,02

Ionic strength of solution: 0,04

$$0{,}04 = \frac{1}{2}[C_{NaCl} * (+1)^2 + C_{NaCl} * (-1)^2 + C_{CaCl2} * (+2)^2 + 2 * C_{CaCl2} * (-1)^2]$$

Solved for CaCl2:

$$0{,}04 = \frac{1}{2}[45 * C_{CaCl2} + 45 * C_{CaCl2} + 4 * C_{CaCl2} + 2 * C_{CaCl2}]$$

$$0{,}04 = \frac{1}{2}[96 * C_{CaCl2}]$$

$$\boldsymbol{C_{CaCl2} = 8,33 * 10^{-4} M}$$

$$\boldsymbol{C_{NaCl} = 0,0375\ M}$$

High salinity solution:

Ionic strength of sample: 0,6

Ionic strength of solution:1,2

$$\boldsymbol{C_{NaCl} = 1,2\ M}$$

High Salinity solution with calcium:

Ratio NaCl/CaCl2 = 1:45

Ionic strength of sample: 0,6

Ionic strength of solution: 1,2

Concentration = 30* Low salinity with calcium:

$$C_{CaCl2} = 8{,}33 * 10^{-4} M * 30$$

$$\boldsymbol{C_{CaCl2} = 0,02499M}$$

$$C_{NaCl} = 0{,}0375\ M * 30$$

$$\boldsymbol{C_{NaCl} = 1,125M}$$

Appendix I: table of PH

Low Salinity:

Low Salinity	Surfactant Concentration [M]	pH before added kaolinite	pH with kaolinite, +36 hours
pH001	10^-3	6,9	6,8
pH002	5*10^-4	6,8	6,9
pH003	10^-4	6,7	6,5
pH004	5*10^-5	6,7	6,5
pH005	10^-5	6,4	5,4

Low Salinity with Calcium:

Low Salinity with calcium	Surfactant Concentration [M]	pH before added kaolinite	pH with kaolinite, +36 hours
pH011	10^-3	6,8	6,8
pH012	5*10^-4	6,9	6,8
pH013	10^-4	6,8	6,7
pH014	5*10^-5	6,7	6,7
pH015	10^-5	6,6	5,7

High Salinity:

High Salinity	Surfactant Concentration [M]	pH before added kaolinite	pH with kaolinite, +36 hours
pH021	5*10^-5	6,5	6,3
pH022	10^-5	5,7	6,4
pH023	5*10^-6	6,6	6,4
pH024	10^-6	6,7	6,6
pH025	5*10^-7	5,6	6,3

High Salinity with Calcium:

High Salinity with calcium	Surfactant Concentration [M]	pH before added kaolinite	pH with kaolinite, +36 hours
pH031	5*10^-5	6,6	6,5
pH032	10^-5	6,4	6,3
pH033	5*10^-6	6,6	6,5
pH034	10^-6	6,6	6,5
pH035	5*10^-7	6,8	6,6